

Non-zero temperature transport near fractional quantum Hall critical points

Subir Sachdev

Department of Physics, P.O. Box 208120, Yale University, New Haven, CT 06520-8120

(October 24, 2018)

Abstract

In an earlier work, Damle and the author (Phys. Rev. B in press; cond-mat/9705206) demonstrated the central role played by incoherent, inelastic processes in transport near two-dimensional quantum critical points. This paper extends these results to the case of a quantum transition in an anyon gas between a fractional quantized Hall state and an insulator, induced by varying the strength of an external periodic potential. We use the quantum field theory for this transition introduced by Chen, Fisher and Wu (Phys. Rev. B **48**, 13749 (1993)). The longitudinal and Hall conductivities at the critical point are both e^2/h times non-trivial, fully universal functions of $\hbar\omega/k_B T$ (ω is the measuring frequency). These functions are computed using a combination of perturbation theory on the Kubo formula, and the solution of a quantum Boltzmann equation for the anyonic quasiparticles and quasiholes. The results include the values of the d.c. conductivities ($\hbar\omega/k_B T \rightarrow 0$); earlier work had been restricted strictly to $T = 0$, and had therefore computed only the high frequency a.c. conductivities with $\hbar\omega/k_B T \rightarrow \infty$.

I. INTRODUCTION

The remarkably rich zero temperature phase diagram of a two-dimensional electron gas in a high magnetic field [1] offers an ideal laboratory for exploring the physics of systems near a quantum critical point. Much theoretical and experimental attention has focussed on the transitions between the various quantum Hall plateau states and the insulator [2,3].

The vast majority of the theoretical work has studied transitions between integer quantum Hall plateaus using a model of non-interacting electrons undergoing phase-coherent transport in the presence of a random potential [2,4]: this transport can be described by non-linear sigma model field theories [5] or by a network model [6]. In this scenario, interactions only provide a phase-breaking length which cuts off the critical quantum interference effects, but are irrelevant perturbations at the quantum-critical point. It has also been suggested that the transitions involving fractional quantum Hall plateaus can be described using closely related models of non-interacting composite fermions [7–9].

However, there have been a number of indications in recent experiments that interactions play a more fundamental role [3,10,11]. Measurements of the non-linear transport [12,3] have allowed direction measurement of the dynamic critical exponent z : the measured value $z \approx 1$ is incompatible with critical points of non-interacting electrons, but can possibly be understood to be a consequence of the Coulomb repulsion at an interacting critical point [13,10]. A more direct indication of the importance comes from measurements of frequency dependent transport. It was found that the width of transition region between the plateaus scales with the same power of frequency, ω , and temperature, T [14]: such a property only holds at quantum transitions described by a fixed point with non-zero interactions, while non-interacting fixed points with irrelevant interactions have very different sensitivities to perturbations in ω and T [15].

Non-zero temperature transport near interacting quantum critical points in two dimensions was studied by Damle and author in a previous paper [11] (hereafter referred to as I). A number of general observations were made, supported by an explicit calculation on the superfluid-insulator transition in a Mott-Hubbard model for bosons. In particular, it was argued that the conductivity at the critical point was given by e^2/h times a non-trivial universal function of the ratio, $\hbar\omega/k_B T$. Attention was drawn to the rather different physical properties of the limiting regimes of frequency and temperature: (i) $\hbar\omega \gg k_B T$ with phase coherent transport of excitations created by the external electric field, and (ii) $\hbar\omega \ll k_B T$, with incoherent, quantum relaxational transport involving repeated inelastic scattering between pre-existing thermally, excited carriers, and relaxation to local equilibrium. The d.c. transport is clearly in the latter regime, and it was noted in I that the d.c. conductivity was universal even though it was dominated by inelastic processes: this was possible because the cross-section for scattering between the carriers became universal at the quantum critical point.

This paper will extend the considerations of I to one of the simplest possible *interacting* quantum critical points in a fractional quantum Hall system. Any experimentally realistic model must account for both the Coulomb interactions among the electrons and for the external random potential. Such a model is of forbidding complexity, and we shall choose here to consider non-random models in the presence of an external *periodic* potential with only a statistical gauge force interaction between the excitations. Our choice is motivated by the

desire to explore seriously the consequences of interactions in the simplest possible context, and the arguments above that inelastic, incoherent processes are essential to any analysis of the experimentally observed critical properties. The absence of a random potential means that there are no localized states: these are essential for the appearance of quantum Hall plateaus as a function of the external magnetic field, as they appear when the Fermi level is in a region of localized states. However, the localized states are not expected to be as crucial in the experimentally relevant critical region (the studies of non-interacting electrons in a random potential examine the complicated physics of the divergence of the localization length at the critical point in perfectly phase coherent transport, but this is always cut off in interacting models at some finite scale due to incoherent, inelastic processes present at any non-zero temperature). A second motivation for examining the case of the periodic potential comes from its importance in the early studies of the integer quantum Hall effect [16]: the topological nature of the quantization of the Hall conductivity first emerged in this context.

A number of earlier studies have examined the fractional quantum Hall effect in a periodic potential. Kol and Read [17] examined general global criteria that must be satisfied by such states. Wen and Wu [18] and Chen, Fisher and Wu [19] first examined the quantum critical points between different fractional quantum Hall states and the insulator, and developed a low energy field-theoretic descriptions of the transitions. They argued that these transitions could be understood in terms of a Mott transition of an anyon gas in a periodic potential and an external magnetic field. The field theory of the anyon gas consisted of a $U(1)$ Chern-Simons gauge field coupled to either relativistic bosonic or Dirac Fermi fields. In an interesting recent work, Pfannkuche and MacDonald [20] have numerically shown the presence of a transition between a fractional quantum Hall state and an insulator induced by varying the strength of an external periodic potential acting on an electron gas in a strong magnetic field: they also present evidence for scaling behavior in the spectrum of small systems near the critical point.

This paper shall describe the nature of non-zero T and ω transport in the $U(1)$ Chern-Simons gauge field coupled to Dirac Fermi field model of Chen, Fisher and Wu [19]. Our motivation for choosing this particular model is mainly technical: it provides the simplest possible context for describing the physics of incoherent transport in quantum Hall critical points, and allows us to keep technical details to a minimum. Our results can also be extended to models of bosons coupled to a Chern-Simons gauge field using a $1/N$ expansion, and this will be discussed in Appendix A. We will show that at the critical point, the longitudinal (σ_{xx}) and Hall (σ_{xy}) conductivities obey the scaling forms

$$\sigma_{xx} = \frac{e^2}{h} \Sigma_{xx} \left(\frac{\hbar\omega}{k_B T} \right) \quad ; \quad \sigma_{xy} = \frac{e^2}{h} \Sigma_{xy} \left(\frac{\hbar\omega}{k_B T} \right) \quad (1.1)$$

We shall extend the quantum transport theory of I to obtain explicit expressions for the universal functions Σ_{xx} and Σ_{xy} . The earlier computations of these conductivities [19] were carried out precisely at $T = 0$, and therefore yielded the values of $\Sigma_{xx}(\infty)$ and $\Sigma_{xy}(\infty)$ which describe phase-coherent transport. The d.c. conductivities are however given by $\Sigma_{xx}(0)$ and $\Sigma_{xy}(0)$: these are quite different, but also universal numbers, characterizing incoherent, relaxational transport, and will be computed in this paper.

As many of the considerations of this paper are similar to those of I, we now explicitly point out some aspects which are different. The central focus of our analysis shall not be

the conductivities σ , but related irreducible conductivities $\tilde{\sigma}$: these are diagrammatically defined as being irreducible towards cutting any single Chern-Simons gauge field propagator. We shall find that many of the issues arising in the computation of $\tilde{\sigma}_{xx}$ are similar to those discussed in I: the focus shall be on a quasiparticle-quasihole contribution which is dominated by collisions among the excitations, and is best described by a quantum transport equation. The physics going into the computation of $\tilde{\sigma}_{xy}$ is quite different. The real part of $\tilde{\sigma}_{xy}$ is non-dissipative and is actually best computed by a simple perturbation theory, which already yields a result which is an interesting function of $\hbar\omega/k_B T$. Indeed, such a perturbation theory was presented in Ref [19] at $T = 0$, and here we consider the orders of limit of $\omega \rightarrow 0$ and $T \rightarrow 0$ more carefully. Our final results for σ_{xx} also has a form rather different from that obtained in I: it is given by complicated interplay between different contributions to $\tilde{\sigma}$: in particular we find that in the low frequency collision-dominated regime it is possible to have σ_{xx} be an increasing, rather than decreasing, function of $\hbar\omega/k_B T$. For the latter situation we find that $\sigma_{xx}(\omega)$ has a peak at $\omega \sim k_B T/\hbar$, and eventually decreases for large enough ω .

As noted above, an essential ingredient in our computation is the quantum transport equation for quasiparticles and quasiholes. These excitations are anyons, and so their scattering cross-section is singular in the forward direction: for momentum transfer q , the cross-section $\sim 1/q^2$ [21]. This scattering cross-section appears in the collision term of the transport equation, and could potentially cause infrared divergences. However we shall show explicitly that the potential divergences all cancel, and the physical transport co-efficients of the anyon gas are well defined. This is an important, albeit technical, consistency check of our analysis, and occupies a significant part of Section IV.

The outline of the remainder of the paper is as follows. We will introduce the model and discuss some important general issues in Section II. The perturbation theory for $\tilde{\sigma}$ will be presented in Section III: this will allow us to identify the different physical contributions to $\tilde{\sigma}$. One of these, the quasiparticle/quasihole contribution is a delta function at zero frequency at leading order in α . This is an artifact, and has to be repaired by an infinite order resummation: the latter is most conveniently carried out using a quantum transport equation analysis which will be discussed in Section IV. We will synthesize our results for $\tilde{\sigma}$ into those for the physically observable σ in Section V, and conclude with some general remarks in Section VI.

II. THE MODEL AND SOME GENERAL CONSIDERATIONS

To the extent possible, we will follow the notation of Ref [19]. We will be working the relativistic models with a velocity c , and use units with $\hbar = c = k_B = 1$, except where we explicitly quote conductivities in units of e^2/h . The imaginary time action of Dirac fermions coupled to a $U(1)$ Chern-Simons gauge field introduced in Ref [19] is

$$\mathcal{S} = \int_0^{1/T} d\tau \int d\mathbf{x} \left\{ \bar{\psi}_1 [\gamma_\mu (\partial_\mu - iqa_\mu - iqeA_\mu) + iM_1] \psi_1 + \bar{\psi}_2 [\gamma_\mu (\partial_\mu - iqa_\mu - iqeA_\mu) + iM_2] \psi_2 + \frac{i}{2} \epsilon_{\mu\nu\lambda} a_\mu \partial_\nu a_\lambda \right\} \quad (2.1)$$

where $\mathbf{x} \equiv (x, y)$, and the Greek indices extend over x, y, τ . The Chern-Simons gauge field is a_μ , the external vector potential driving the currents in A_μ , and $\psi_{1,2}$ are two species of Dirac fermions with charge qe . The Dirac matrices are $\gamma_\mu = i(-\tau_y, \tau_x, \tau_z)$ where τ are the Pauli matrices, and $\bar{\psi} = \psi^\dagger \gamma_\tau$. Notice that we are using the symbol τ to indicate both imaginary time and the Pauli matrices, but the meaning should be clear from the context. The sole role of a_μ and the Chern-Simons term is to attach flux tubes onto each Dirac fermion and to convert it to a Dirac anyon with statistics parameter $(1 - \alpha)$ where

$$\alpha = \frac{g^2}{2\pi}; \quad (2.2)$$

we are using the nomenclature where a statistics parameter of 1 corresponds to fermions, and 0 to bosons. Notice that we have two species of anyons, $\psi_{1,2}$: these are required by the doubling theorems for chiral fermions on a lattice. The anyons/anti-anyons represent the Laughlin quasiparticles/quasiholes of the fractional quantized Hall state. So to describe physics in the vicinity of the simplest Laughlin quantum Hall state at filling $\nu = 1/3$ we should choose $\alpha = 2/3$ and $q = 1/3$. As we will review below, the action \mathcal{S} describes [19] a quantum transition between fractional quantized Hall state with $T = 0$ conductivity (the Latin indices extend over x, y)

$$\sigma_{ij} = -\epsilon_{ij} \frac{e^2}{h} \frac{q^2}{(1 - \alpha)} \quad (2.3)$$

and an insulator with $\sigma_{ij} = 0$. Notice that, as expected, (2.3) gives a Hall conductance of $e^2/(3h)$ for $q = 1/3$ and $\alpha = 2/3$.

We now make some general remarks about the nature of charge transport in Chern-Simons theories: these results are well known [8,19], but our formulation is especially suited to our subsequent analysis of inelastic processes using the quantum Boltzmann equation.

From the equation of motion of a_μ implied by \mathcal{S} , we see that role of a_μ is to impose the constraint

$$\epsilon_{\mu\nu\lambda} \partial_\nu a_\lambda = g (\bar{\psi}_1 \gamma_\mu \psi_1 + \bar{\psi}_2 \gamma_\mu \psi_2). \quad (2.4)$$

This constraint will be imposed *exactly* in all stages of our analysis. The τ component of this constraint is

$$\epsilon_{ij} \partial_i a_j = -g (\psi_1^\dagger \psi_1 + \psi_2^\dagger \psi_2). \quad (2.5)$$

where the Latin indices extend over x, y . The spatial components of (2.4) can be written as

$$-qe\epsilon_{ij} E_{aj} = g (J_{1i} + J_{2i}) \quad (2.6)$$

where \mathbf{E}_a is the ‘electric field’ associated with the a_μ gauge field

$$E_{ai} = \partial_\tau a_i - \partial_i a_\tau, \quad (2.7)$$

and $\mathbf{J}_1, \mathbf{J}_2$ are the electrical currents carried by the two species of Dirac fermions:

$$J_{1i} = qe\bar{\psi}_1\gamma_i\psi_1 \quad (2.8)$$

and similarly for \mathbf{J}_2 .

We shall be interested in the response of \mathcal{S} to an external physical electric field \mathbf{E} given, of course, by

$$E_i = \partial_\tau A_i - \partial_i A_\tau, \quad (2.9)$$

The currents induced by such a field, in turn, induce a non-zero value of the \mathbf{E}_a field, by (2.6). It is therefore useful to define

$$\mathbf{E}_T = \mathbf{E} + \frac{g}{qe}\mathbf{E}_a \quad (2.10)$$

as the *total* effective field experienced by the Dirac fermions. The field \mathbf{E}_T will appear naturally in our subsequent formulation of the quantum transport equations. It is then useful to consider the response of the fermions by introducing the linear response relations

$$J_{1i}(\omega) = \tilde{\sigma}_{1ij}(\omega)E_{Tj}(\omega) \quad (2.11)$$

and similarly for \mathbf{J}_2 . We have also introduced a frequency ω to allow for the response to a time-dependent electric field. In diagrammatic terms, if we compute $\tilde{\sigma}_\pm$ via a Kubo formula, we should only include diagrams which are irreducible towards cutting any a_μ propagator: the irreducibility requirement is equivalent to considering the response to the effective field \mathbf{E}_T .

The experimentally measured response, σ_{ij} , of course, relates the total current to the external electric field

$$J_{1i}(\omega) + J_{2i}(\omega) = \sigma_{ij}(\omega)E_j(\omega) \quad (2.12)$$

From (2.6,2.10,2.11,2.12) we can obtain the following basic relationship [8,19] between the response functions

$$(\sigma^{-1})_{ij} = (\tilde{\sigma}_1 + \tilde{\sigma}_2)_{ij}^{-1} - \frac{h}{q^2 e^2} \epsilon_{ij} \alpha. \quad (2.13)$$

When we are well away from the critical point, $|M_{1,2}|$ is large, and the $\sigma_{1,2}$ are easily computed at $T = 0$; their exact values are [19]

$$\tilde{\sigma}_{1,2} = -\frac{q^2 e^2}{2h} \epsilon_{ij} \text{sgn}(M_{1,2}). \quad (2.14)$$

We see therefore that with the choices $M_1 > 0$ and $M_2 > 0$, (2.13,2.14) lead to the conductivity (2.3) of the fractional quantized Hall state. The system undergoes a transition to an insulator if M_1 changes sign while M_2 remains positive: then the total conductivity vanishes.

The remainder of the paper will study the critical point where M_2 is large and positive (and therefore the ψ_2 fermionic excitations have large gap) while the renormalized $M_1 = 0$ at $T = 0$. The $\tilde{\sigma}_2$ conductivity therefore continues to satisfy (2.14) at all low T and ω ; all

corrections are suppressed by factors of $e^{-M_2/T}$. The response of the ψ_1 fermions is much more non-trivial, and will occupy the remainder of the paper to elucidate: it has a highly non-trivial, universal function of ω/T . As our attention will focus solely on the response of the ψ_1 fermions, we will henceforth drop the subscript 1, and simply refer to them as the ψ fermions.

The central purpose of this paper is to analyze the quantum transport properties of the model \mathcal{S} in (2.1) at $T > 0$. While the action \mathcal{S} is Lorentz invariant, the presence of a nonzero T breaks the Lorentz symmetry, and the space and time dependence of observable correlators will be quite different. Therefore, there is no particular advantage to working with a covariant gauge, and it pays to choose a gauge better suited to physics at $T > 0$. It turns out that by far the most convenient choice is the Coulomb gauge: the perturbative calculations to be considered in Section III are the most straightforward, and the quantum transport equations of Section IV are readily derived in this gauge. The Coulomb gauge corresponds to the choice

$$\partial_i a_i = 0, \quad (2.15)$$

combined with an exact integral of \mathcal{S} over a_τ . Then the constraint (2.5) can be solved to give

$$a_i = g \frac{\epsilon_{ij} \partial_j}{\partial^2} \psi^\dagger \psi \quad (2.16)$$

where $\partial^2 \equiv \partial_i \partial_i$. Note that this is an equal-time relationship—the absence of retardation in the gauge field interactions is an important simplifying feature of this gauge. Inserting (2.16) into (2.1) (and dropping the non-critical ψ_2 fermions) we obtain the Hamiltonian density

$$H = H_0 + H_1$$

$$H_0 = \int d\mathbf{x} \left[\psi^\dagger (-i\tau_i \partial_i - M_0 \tau_z) \psi \right] \quad (2.17)$$

$$H_1 = \int d\mathbf{x} \left[2\pi\alpha \psi^\dagger \epsilon_{ij} \tau_j \psi \frac{\partial_i}{\partial^2} \psi^\dagger \psi \right]. \quad (2.18)$$

We have inserted a *bare* mass M_0 in H_0 ; to ensure that the system is at its critical point, the value of M_0 will have to be adjusted order by order in α so that the *renormalized* mass vanishes at $T = 0$. Note that the gauge field has disappeared as an independent dynamical degree of freedom: each Dirac particle/anti-particle now has a flux tube attached, and it is this flux tube which is responsible for the long-range force in H_1 . This economical description of the degrees of freedom will be quite useful when we consider the transport equation at nonzero temperature.

The remainder of the computations in this paper will be carried out using the Hamiltonian H .

III. PERTURBATION THEORY AND KUBO FORMULA

We will begin in Section III A, as in the analysis for the bosonic case in I and in Ref [22], by an examination of the perturbative structure of the single particle self energy. Then,

we will proceed in Sections III B and III C to an evaluation of $\tilde{\sigma}_{xx}$ and $\tilde{\sigma}_{xy}$ using the Kubo formula. We will gain an understanding of the physically different contributions to $\tilde{\sigma}$ by examining the structure of the bare perturbation theory in powers of α . The results for $\tilde{\sigma}$ will have some unphysical features which will finally be rectified by an analysis using the quantum Boltzmann equation in the following Section IV.

A. Self energy

The purpose of this section is to understand the structure of the mass renormalization in a single fermion propagator. As noted earlier, we need to adjust the value of M_0 so that the renormalized mass vanishes at $T = 0$. However the renormalized mass need not vanish at $T > 0$, and we will describe its universal T dependence here. We will denote the renormalized mass by $M(T)$, and clearly we should have $M(0) = 0$.

To leading order in α , it turns out to be sufficient to consider evaluation of $M(T)$ in a bare perturbation theory in α , without the need for any self-consistent mass renormalization; the latter only modify results at higher orders in α . As M_0 is expected to be of order α , we may therefore set $M_0 = 0$ within the propagators that appear in the self energy. To first order in α , the fermion self energy for H is

$$\Sigma(\mathbf{k}) = 2\pi\alpha i\epsilon_{ij}T \sum_{\epsilon_n} \int \frac{d^2p}{(2\pi)^2} \frac{(k_i - p_i)}{(\mathbf{k} - \mathbf{p})^2} \text{Tr} \left(\frac{1}{-i\epsilon_n + \mathbf{p} \cdot \vec{\tau}} \tau_j - \tau_j \frac{1}{-i\epsilon_n + \mathbf{p} \cdot \vec{\tau}} \right). \quad (3.1)$$

The trace is over the Dirac spinor space, ϵ_n is a fermionic Matsubara frequency, and to this order, Σ is independent of the fermion frequency. Evaluating the trace and performing the frequency summation, we get

$$\Sigma(\mathbf{k}) = -\pi\alpha\tau_z \int \frac{d^2p}{(2\pi)^2} \frac{(\mathbf{k} - \mathbf{p}) \cdot \mathbf{p}}{p(\mathbf{k} - \mathbf{p})^2} \tanh(p/2T) \quad (3.2)$$

The leading τ_z shows that $\Sigma(0)$ is precisely a mass renormalization, and therefore

$$M(T) = M_0 + \Sigma(0)|_{T=0}. \quad (3.3)$$

Using $M(0) = 0$, we get

$$M_0 = -2\pi\alpha \int^{\Lambda} \frac{d^2p}{(2\pi)^2} \frac{1}{p} \quad (3.4)$$

where Λ is an ultraviolet momentum cutoff, whose nature we will not have to precisely specify. Finally, inserting (3.4) and (3.2) into (3.3) we get

$$M(T) = -4\pi\alpha \int \frac{d^2p}{(2\pi)^2} \frac{f^0(p)}{p} \quad (3.5)$$

where $f^0(p)$ is the Fermi function

$$f^0(p) = \frac{1}{e^{p/T} + 1}. \quad (3.6)$$

The integral in (3.5) is easily evaluated, and we get our final result

$$M(T) = -2\alpha T \ln(2). \quad (3.7)$$

We will find later that in some cases it is necessary to include this renormalized mass in the fermion propagators, while in other cases we will simply be able to use the zeroth order result $M(T) = 0$.

B. $\tilde{\sigma}_{xx}$

The leading contribution to $\tilde{\sigma}_{xx}$ is given by a single fermion polarization bubble, with the mass $M(T)$ above included in the propagators. To first order in α there are three additional diagrams, considered in Ref [19], which contribute to the conductivity; however, these only yield contributions to $\tilde{\sigma}_{xy}$ and will be discussed in Section III C. The fermion polarization contribution to $\tilde{\sigma}_{xx}$ is

$$\begin{aligned} \tilde{\sigma}_{xx}(i\omega_n) = \frac{2\pi q^2 e^2}{h\omega_n} T \sum_{\epsilon_n} \int \frac{d^2 k}{(2\pi)^2} \text{Tr} \left(\tau_x \frac{1}{(-i\epsilon_n + \mathbf{k} \cdot \vec{\tau} - M(T)\tau_z)} \right. \\ \left. \times \tau_x \frac{1}{(-i(\epsilon_n + \omega_n) + \mathbf{k} \cdot \vec{\tau} - M(T)\tau_z)} \right). \end{aligned} \quad (3.8)$$

The trace is over the Dirac spinor space, and evaluating it and simplifying a bit, we obtain

$$\tilde{\sigma}_{xx}(i\omega_n) = \frac{2\pi q^2 e^2}{h\omega_n} T \sum_{\epsilon_n} \int \frac{d^2 k}{(2\pi)^2} \left[\frac{4k_x^2 + \omega_n^2}{(\varepsilon_k^2 + \epsilon_n^2)(\varepsilon_k^2 + (\epsilon_n + \omega_n)^2)} - \frac{2}{\varepsilon_k^2 + \epsilon_n^2} \right] \quad (3.9)$$

where

$$\varepsilon_k^2 \equiv k^2 + M^2(T) \quad (3.10)$$

The two terms in the integrand in (3.9) cancel at $T = 0$ in the $\omega_n \rightarrow 0$ limit, but this is not evident in the present form. To make this explicit, insert $1 = \partial k_x / \partial k_x$ in front of the second term, and integrate by parts under the k_x integral; this yields

$$\tilde{\sigma}_{xx}(i\omega_n) = \frac{2\pi q^2 e^2}{h\omega_n} T \sum_{\epsilon_n} \int \frac{d^2 k}{(2\pi)^2} \frac{1}{(\varepsilon_k^2 + \epsilon_n^2)} \left[\frac{4k_x^2 + \omega_n^2}{(\varepsilon_k^2 + (\epsilon_n + \omega_n)^2)} - \frac{4k_x^2}{\varepsilon_k^2 + \epsilon_n^2} \right]. \quad (3.11)$$

We can now evaluate the summation over ϵ_n and analytically continue the result to real ω ; as in I it is convenient to separate the result into two distinct pieces

$$\tilde{\sigma}_{xx}(\omega) \equiv \tilde{\sigma}_{xx}^{\text{qp}}(\omega) + \tilde{\sigma}_{xx}^{\text{coh}}(\omega). \quad (3.12)$$

The first piece, $\tilde{\sigma}_{xx}^{\text{qp}}(\omega)$, is the contribution of thermally excited quasiparticles:

$$\begin{aligned} \tilde{\sigma}_{xx}^{\text{qp}}(\omega) &= \delta_{ij} \frac{4\pi q^2 e^2}{h} \left[\pi\delta(\omega) + i\mathcal{P}\left(\frac{1}{\omega}\right) \right] \int \frac{d^2 k}{(2\pi)^2} \frac{k_x^2}{\varepsilon_k^2} \left(-\frac{\partial f^0(\varepsilon_k)}{\partial \varepsilon_k} \right) \\ &= \frac{q^2 e^2 \mathcal{N}(\alpha)}{h} \left[\pi\delta(\omega/T) + i\mathcal{P}\left(\frac{T}{\omega}\right) \right], \end{aligned} \quad (3.13)$$

where $\mathcal{N}(\alpha)$, obtained after using (3.7), is a pure number

$$\begin{aligned}\mathcal{N}(\alpha) &\equiv \int_{2\alpha \ln 2}^{\infty} dy \frac{y^2 - 4\alpha^2 \ln^2(2)}{4y \cosh^2(y/2)} \\ &= \ln(2) + \mathcal{O}(\alpha^2)\end{aligned}\quad (3.14)$$

At this order, this contribution to the real part of the conductivity is simply a delta function of frequency of weight $\propto T$ (which satisfies the scaling form (1.1)). A more sophisticated quantum transport analysis (of the type carried out in I), to be discussed in the next section, will show how this delta function is broadened out by inelastic, incoherent collisions that appear at higher orders in α . The second piece, $\tilde{\sigma}^{\text{coh}}(\omega)$ is a smooth continuum contribution from the creation of quasi-particle/quasi-hole pairs by the external source, to the real part of the conductivity, and contains the coherent contribution in the limit $\omega/T \rightarrow \infty$; after a change of variables in the momentum integration from k to ε_k , it can be written as

$$\tilde{\sigma}_{xx}^{\text{coh}}(\omega) = \frac{q^2 e^2}{2h} \int_{|M(T)|}^{\infty} d\varepsilon_k \frac{-i\omega(\varepsilon_k^2 + M^2(T)) \tanh(\varepsilon_k/2T)}{\varepsilon_k(4\varepsilon_k^2 - (\omega + i\eta)^2)}, \quad (3.15)$$

where η is a positive infinitesimal. The real part of this result can be evaluated in closed form

$$\text{Re} [\tilde{\sigma}_{xx}^{\text{coh}}(\omega)] = \frac{\pi q^2 e^2}{8h} \theta(|\omega| - 2M(T)) \left(1 + \frac{4M^2(T)}{\omega^2}\right) \tanh(|\omega|/4T), \quad (3.16)$$

while the imaginary part can be obtained by a Kramers-Kronig transform of $\text{Re} [\tilde{\sigma}_{xx}^{\text{coh}}(\omega)] - \pi q^2 e^2 / 8h$. Note that, after using (3.7) for $M(T)$, the result (3.15) is consistent with the scaling form (1.1). We show a plot of the frequency dependence of the real and imaginary parts of $\tilde{\sigma}_{xx}^{\text{coh}}$ in Fig 1. There are weak threshold singularities at $\omega = 2M(T)$: a discontinuity in $\text{Re} [\tilde{\sigma}_{xx}]$ and a corresponding logarithmic divergence in $\text{Im} [\tilde{\sigma}_{xx}]$. These are artifacts of the absence of damping in the fermion propagators at this order, and the singularities are expected to be smoothed out at higher orders.

The previous computation of $\text{Re} [\tilde{\sigma}_{xx}]$ in Ref [19] was carried out at $T = 0$, in which we obtain only the $\omega/T \rightarrow \infty$ limit of $\tilde{\sigma}^{\text{coh}}$ which, from (3.15), is given by

$$\tilde{\sigma}_{xx}(\omega/T \rightarrow \infty) = \pi q^2 e^2 / 8h. \quad (3.17)$$

In the limit $\omega/T \rightarrow 0$ relevant to d.c. transport, $\tilde{\sigma}_{xx}$ is dominated by $\tilde{\sigma}_{xx}^{\text{qp}}$, which at this order is a delta function at zero frequency: as stated earlier, this will be repaired in Section IV by a quantum transport analysis.

C. $\tilde{\sigma}_{xy}$

Unlike $\tilde{\sigma}_{xx}$, the zeroth order in α result for $\tilde{\sigma}_{xy}$ vanishes identically at the critical point. It is necessary to go to first order in α , where one finds two distinct types of contributions. The first (denoted $\tilde{\sigma}_{xy}^{(1)}$) comes from the simple fermion polarization bubble considered above for $\tilde{\sigma}_{xx}$, but with the first order result for the mass $M(T)$ in (3.7) included. The second comes

from the diagrams, considered in Ref. [19], which are explicitly first order in α : these account for the momentum dependence of the self-energy (denoted $\tilde{\sigma}_{xy}^{(2)}$) and the corresponding vertex correction (denoted $\tilde{\sigma}_{xy}^{(3)}$).

Considering first the contribution of the simple polarization bubble. This gives

$$\begin{aligned} \tilde{\sigma}_{xy}^{(1)}(i\omega_n) &= \frac{2\pi q^2 e^2}{h\omega_n} T \sum_{\epsilon_n} \int \frac{d^2 k}{(2\pi)^2} \text{Tr} \left(\tau_x \frac{1}{(-i\epsilon_n + \mathbf{k} \cdot \vec{\tau} - M(T)\tau_z)} \right. \\ &\quad \left. \times \tau_y \frac{1}{(-i(\epsilon_n + \omega_n) + \mathbf{k} \cdot \vec{\tau} - M(T)\tau_z)} \right). \end{aligned} \quad (3.18)$$

Evaluating the Dirac trace and the frequency summation, we find that the leading $1/\omega_n$ explicitly cancels out: as a result there will be no singular $\delta(\omega)$ contributions to $\tilde{\sigma}_{xy}$ as there were to $\tilde{\sigma}_{xx}$. We change variables in the momentum integration from k to ϵ_k , and analytically continue to real frequencies, and the answer takes the final form

$$\tilde{\sigma}_{xy}^{(1)}(\omega) = -\frac{2q^2 e^2 M(T)}{h} \int_{|M(T)|}^{\infty} d\epsilon_k \frac{\tanh(\epsilon_k/2T)}{4\epsilon_k^2 - (\omega + i\eta)^2} \quad (3.19)$$

Notice that there is $M(T)$ in the prefactor, and so this result is at least first order in α . Nevertheless, it is not permissible to simply set $M(T) = 0$ in the lower limit of the integration to obtain the leading result: this is because the integrand has a potential logarithmic divergence for $\omega_n = 0$, which is cutoff by the lower limit. The result (3.19) vanishes as $\sim iT/\omega$ in the limit $\omega/T \rightarrow \infty$, while in the d.c. limit $\omega/T \rightarrow 0$ we get after using (3.7) and manipulations described in Appendix B:

$$\begin{aligned} \tilde{\sigma}_{xy}^{(1)}(\omega/T \rightarrow 0) &= \frac{q^2 e^2}{h} \left[\left(\frac{\ln(2)}{2} \right) \alpha \ln(1/\alpha) \right. \\ &\quad \left. + \frac{\ln(2)}{6} \{3 - 3\gamma - 7\ln(2) - 3\ln(\ln(2)) - 36\zeta'(-1)\} \alpha + \mathcal{O}(\alpha^3) \right] \end{aligned} \quad (3.20)$$

Here $\gamma = 0.5772\dots$ is Euler's constant and $\zeta(s)$ is the Riemann zeta function. Notice the non-analytic $\alpha \ln(1/\alpha)$ term: the proper T dependence of the mass $M(T)$ discussed in Section III A was required to obtain this.

We now consider the three diagrams for $\tilde{\sigma}$ which are explicitly first order in α . These were considered in Ref [19] at $T = 0$; the $T > 0$ calculations are forbiddingly complicated in the Lorentz gauge used in Ref [19] because of the retardation in the gauge field propagator; they simplify considerably in the Coulomb gauge we are using here. To first order in α we can set $M(T) = 0$ in the propagators of these diagrams; this is justified *a posteriori* by the absence of infrared divergences in our evaluation of these diagrams. The first such contribution is the sum of the two diagrams accounting for the momentum dependence of the self-energy correction in one of the fermion propagators:

$$\begin{aligned} \tilde{\sigma}_{xy}^{(2)}(i\omega_n) &= \frac{8\pi^2 q^2 e^2 \alpha}{h\omega_n} i\epsilon_{ij} T \sum_{\epsilon_n} \int \frac{d^2 k}{(2\pi)^2} \frac{d^2 p}{(2\pi)^2} \left[\frac{(k_i - p_i)}{(\mathbf{k} - \mathbf{p})^2} + \frac{p_i}{p^2} \right] \\ &\quad \times \text{Tr} \left[\tau_x \frac{1}{(-i\epsilon_n + \mathbf{k} \cdot \vec{\tau})} \left\{ \frac{1}{(-i\Omega_n + \mathbf{p} \cdot \vec{\tau})} \tau_j - \tau_j \frac{1}{(-i\Omega_n + \mathbf{p} \cdot \vec{\tau})} \right\} \right. \\ &\quad \left. \frac{1}{(-i\epsilon_n + \mathbf{k} \cdot \vec{\tau})} \tau_y \frac{1}{(-i(\epsilon_n + \omega_n) + \mathbf{k} \cdot \vec{\tau})} \right] \end{aligned} \quad (3.21)$$

The second term in the first square bracket is the subtraction that corrects for the momentum-independent mass renormalization that was already accounted for by including a $M(T)$ in $\tilde{\sigma}_{xy}^{(1)}$. The final contribution to $\tilde{\sigma}_{xy}$ is the first-order vertex correction corresponding to the self-energy in $\tilde{\sigma}_{xy}^{(2)}$:

$$\begin{aligned} \tilde{\sigma}_{xy}^{(3)}(i\omega_n) &= \frac{4\pi^2 q^2 e^2 \alpha}{\hbar\omega_n} i\epsilon_{ij} T^2 \sum_{\epsilon_n, \Omega_n} \int \frac{d^2 k}{(2\pi)^2} \frac{d^2 p}{(2\pi)^2} \frac{(k_i - p_i)}{(\mathbf{k} - \mathbf{p})^2} \\ &\times \text{Tr} \left[\tau_x \frac{1}{(-i\epsilon_n + \mathbf{k} \cdot \vec{\tau})} \left\{ \frac{1}{(-i\Omega_n + \mathbf{p} \cdot \vec{\tau})} \tau_y \frac{1}{(-i(\Omega_n + \omega_n) + \mathbf{p} \cdot \vec{\tau})} \tau_j \right. \right. \\ &\left. \left. - \tau_j \frac{1}{(-i\Omega_n + \mathbf{p} \cdot \vec{\tau})} \tau_y \frac{1}{(-i(\Omega_n + \omega_n) + \mathbf{p} \cdot \vec{\tau})} \right\} \frac{1}{(-i(\epsilon_n + \omega_n) + \mathbf{k} \cdot \vec{\tau})} \right] \end{aligned} \quad (3.22)$$

We now evaluate the trace over Dirac indices, sum over frequencies in (3.21) and analytically continue to real frequencies to obtain:

$$\begin{aligned} \tilde{\sigma}_{xy}^{(2)}(\omega) &= -\frac{8\pi^2 q^2 e^2 \alpha}{h} \int \frac{d^2 k}{(2\pi)^2} \frac{d^2 p}{(2\pi)^2} \frac{\tanh(p/2T) \tanh(k/2T)}{pk(4k^2 - (\omega + i\eta)^2)} \left(\frac{(p^2 - \mathbf{k} \cdot \mathbf{p})}{(\mathbf{k} - \mathbf{p})^2} - 1 \right) \\ &= \frac{2q^2 e^2 \alpha}{h} \int_0^\infty dp \int_p^\infty dk \frac{\tanh(p/2T) \tanh(k/2T)}{(4k^2 - (\omega + i\eta)^2)}, \end{aligned} \quad (3.23)$$

where in the second expression we have evaluated the angular integrals. As discussed in Ref [19], it is important in (3.23) that the k integral be evaluated first as it is convergent. There is a logarithmic divergence in the subsequent p integral but this will cancel against an opposite contribution in $\tilde{\sigma}_{xy}^{(3)}$. The trace and summation over frequencies in (3.22) yields

$$\begin{aligned} \tilde{\sigma}_{xy}^{(3)}(\omega) &= -\frac{32\pi^2 q^2 e^2 \alpha}{h} \int \frac{d^2 k}{(2\pi)^2} \frac{d^2 p}{(2\pi)^2} \frac{(\mathbf{k} \times \mathbf{p})^2}{pk(\mathbf{k} - \mathbf{p})^2} \frac{\tanh(p/2T) \tanh(k/2T)}{(4k^2 - (\omega + i\eta)^2)(4p^2 - (\omega + i\eta)^2)} \\ &= -\frac{4q^2 e^2 \alpha}{h} \int_0^\infty dp \int_0^\infty dk \text{Min}(k^2, p^2) \frac{\tanh(p/2T) \tanh(k/2T)}{(4k^2 - (\omega + i\eta)^2)(4p^2 - (\omega + i\eta)^2)} \end{aligned} \quad (3.24)$$

where again the second expression is obtained after evaluating the angular integrals, and we choose to evaluate the k integral first. The integrals can be evaluated explicitly in the limit $\omega/T \rightarrow \infty$, and we get

$$\tilde{\sigma}_{xy}^{(2)}(\omega/T \rightarrow \infty) + \tilde{\sigma}_{xy}^{(3)}(\omega/T \rightarrow \infty) = \frac{q^2 e^2 \alpha}{h} \frac{(\pi^2 + 4)}{16} \quad (3.25)$$

In the opposite limit, $\omega/T \rightarrow 0$, we evaluated the integrals numerically, and found to a very high accuracy that

$$\tilde{\sigma}_{xy}^{(2)}(\omega/T \rightarrow 0) + \tilde{\sigma}_{xy}^{(3)}(\omega/T \rightarrow 0) = \frac{q^2 e^2 \alpha}{4h}, \quad (3.26)$$

although we have no analytic proof of this simple result. The full frequency dependence is most easily evaluated by first taking the imaginary parts of (3.21) and (3.22), which can be shown to simplify to

$$\text{Im} \left[\tilde{\sigma}_{xy}^{(2)}(\omega) + \tilde{\sigma}_{xy}^{(3)}(\omega) \right] = \frac{q^2 e^2 \pi \alpha}{h} \omega \tanh(|\omega|/4T) \int_0^\infty dp f^0(p/T) \mathcal{P} \left(\frac{1}{4p^2 - \omega^2} \right). \quad (3.27)$$

The real part is obtained by adding the constant $q^2 e^2 \alpha (\pi^2 + 4)/16h$ to the Kramers-Kronig transform of (3.27).

We now combine (3.19), (3.23) and (3.24) to obtain the final results for $\tilde{\sigma}_{xy}$. We have the limiting values

$$\begin{aligned} \tilde{\sigma}_{xy}(\omega/T \rightarrow 0) &= \frac{q^2 e^2}{h} \left[\left(\frac{\ln(2)}{2} \right) \alpha \ln(1/\alpha) + (0.650988\dots) \alpha + \mathcal{O}(\alpha^3) \right] \\ \tilde{\sigma}_{xy}(\omega/T \rightarrow \infty) &= \frac{q^2 e^2}{h} \left[\left(\frac{\pi^2 + 4}{16} \right) \alpha + \mathcal{O}(\alpha^3) \right] \end{aligned} \quad (3.28)$$

The second of these results has been obtained previously [19,23]; that calculation was done in a Lorentz invariant gauge, and it is reassuring that the same result has been obtained here in a completely different, non-relativistic gauge. Notice that there are no delta function contributions to $\tilde{\sigma}_{xy}$: this implies that the entire contribution is due to coherent quasiparticle/quasi-hole creation, and the collisionless flow of pre-existing thermally excited particles/holes contributes only to $\tilde{\sigma}_{xx}^{\text{qp}}$.

We conclude this section by showing a plot of the frequency dependence of the real and imaginary parts of $\tilde{\sigma}_{xy}$ in Fig 2. Notice that, as in $\tilde{\sigma}_{xx}$ there are threshold singularities at $\omega = 2M(T)$: a discontinuity in $\text{Im}[\tilde{\sigma}_{xx}]$ and a corresponding logarithmic divergence in $\text{Im}[\tilde{\sigma}_{xx}]$. Again these artifacts of the absence of damping in the fermion propagators at this order.

IV. QUANTUM TRANSPORT EQUATIONS

The perturbative analysis of $\tilde{\sigma}$ in Section III produced results which had singularities at two frequencies: a delta function in $\tilde{\sigma}_{xx}^{\text{qp}}$ at $\omega = 0$, and much weaker logarithmic singularities at $\omega = 2M(T)$. Both these features are in fact artifacts of the low order results, and disappear when damping of fermion excitations is accounted for at higher orders. In this section, we shall show how the delta function singularity at $\omega = 0$ is broadened out at order α^2 . The singularity at $\omega = 2M(T)$ is due to a threshold to creation of particle-hole pairs: it is also expected to be smoothed out at order α^2 , but determination of the precise form of this is left as an open problem.

So to reiterate, this section will only describe the changes to the result for $\tilde{\sigma}_{xx}^{\text{qp}}$ in (3.13) at higher order in α . The perturbative results for the other pieces of $\tilde{\sigma}$, in particular, (3.15) for $\tilde{\sigma}_{xx}$ and (3.19), (3.23), and (3.24) for $\tilde{\sigma}_{xy}$, will be used unchanged in our subsequent considerations as their spurious singularities are relatively minor.

The delta function singularity in $\tilde{\sigma}_{xx}^{\text{qp}}$, will be explicitly shown below to be due to the collisionless transport of thermally excited quasiparticles and quasiholes. This will be done as in I: by writing down transport equations for the distribution functions of these excitations. The collisionless form of these equations appear in Section IV A and their solution reproduces the result for $\tilde{\sigma}_{xx}^{\text{qp}}$ obtained in Section III B; then, in Section IV B, we include collision terms and present the numerical solution.

A. Collisionless transport of quasiparticles and quasiholes

We begin by recalling the defining relation (2.11) for $\tilde{\sigma}$: it is the linear response in the current to the total internal field \mathbf{E}_T . Fortunately, the field \mathbf{E}_T appears in the transport equation in a simple and natural way: the effect of the Hartree and Fock terms is precisely such as to modify the external field \mathbf{E} to \mathbf{E}_T [24]. As a result we can simply omit these terms while replacing \mathbf{E} by \mathbf{E}_T , and determination of the $\tilde{\sigma}$ becomes, as in I, a matter of balancing the ballistic, particle streaming terms with the collision term.

Throughout Section IV we will work with fermionic excitations with a spectrum $\varepsilon_k = k$ *i.e.* we will set the mass $M(T) = 0$; as the Hartree and Fock terms in the self-energy are also implicitly accounted for in our analysis, this is equivalent to simply disregarding such terms and working with a H_O with $M_0 = 0$. In this approximation the transport analysis will yield a normalization constant for the spectral weight in the conductivity in (3.13) which is given by the result correct to leading order in α , $\mathcal{N}(\alpha) = \ln(2)$. Our objective will then be to describe the broadening of the delta function in (3.13), while omitting all terms which lead to corrections in its total spectral weight.

The simplest formulation of the transport equations is in a basis which diagonalizes the Hamiltonian H_0 . To do this, we first express ψ in its Fourier components

$$\psi(\mathbf{x}, t) = \int \frac{d^2k}{(2\pi)^2} \begin{pmatrix} c_1(\mathbf{k}, t) \\ c_2(\mathbf{k}, t) \end{pmatrix} e^{i\mathbf{k}\cdot\mathbf{x}}, \quad (4.1)$$

and then perform a unitary transformation from the Fourier mode operators (c_1, c_2) to (γ_+, γ_-) :

$$\begin{aligned} c_1(k) &= \frac{1}{\sqrt{2}}(\gamma_+(\mathbf{k}) + \gamma_-(\mathbf{k})) \\ c_2(k) &= \frac{K}{\sqrt{2}k}(\gamma_+(\mathbf{k}) - \gamma_-(\mathbf{k})). \end{aligned} \quad (4.2)$$

We have introduced here a notational convention that we shall find quite useful in the following: as \mathbf{k} is a two-dimensional momentum, we can define the complex number K by

$$K \equiv k_x + ik_y \quad \text{where} \quad \mathbf{k} \equiv (k_x, k_y) \quad (4.3)$$

and $k = |\mathbf{k}| = |K|$. Expressing the Hamiltonian H_0 in terms of γ_\pm , we obtain the simple result

$$H_0 = \sum_{\lambda} \int \frac{d^2k}{(2\pi)^2} \lambda k \gamma_{\lambda}^{\dagger}(\mathbf{k}) \gamma_{\lambda}(\mathbf{k}) \quad (4.4)$$

where the sum over λ extends over $+, -$. So γ_+^{\dagger} creates a particle with energy k , while γ_-^{\dagger} creates a particle with energy $-k$. At zero temperature the negative energy states will be filled: so we identify γ_+^{\dagger} as the creation operator for quasiparticles, while γ_-^{\dagger} is the creation operator for quasiholes. Notice that the quasiparticles and quasiholes are distinct excitations in different bands, and the absence of a quasiparticle is *not* equivalent to the presence of a quasihole: this latter feature was also present in the bosonic analysis of I, and as argued

there, allows the system to acquire a non-zero d.c. resistance while maintaining conservation of total momentum.

Let us also, for future use, express the interaction Hamiltonian H_1 in terms of the γ_{\pm} :

$$H_1 = \sum_{\lambda_1 \lambda_2 \lambda_3 \lambda_4} \int \frac{d^2 k_1}{(2\pi)^2} \frac{d^2 k_2}{(2\pi)^2} \frac{d^2 k_q}{(2\pi)^2} \times T_{\lambda_1 \lambda_2 \lambda_3 \lambda_4}(\mathbf{k}_1, \mathbf{k}_2, \mathbf{q}) \gamma_{\lambda_4}^\dagger(\mathbf{k}_1 + \mathbf{q}) \gamma_{\lambda_3}^\dagger(\mathbf{k}_2 - \mathbf{q}) \gamma_{\lambda_2}(\mathbf{k}_2) \gamma_{\lambda_1}(\mathbf{k}_1) \quad (4.5)$$

where

$$T_{\lambda_1 \lambda_2 \lambda_3 \lambda_4}(\mathbf{k}_1, \mathbf{k}_2, \mathbf{q}) = -\frac{\pi\alpha}{2q^2} \left[1 + \lambda_1 \lambda_4 \frac{(K_1^* + Q^*) K_1}{|\mathbf{k}_1 + \mathbf{q}| k_1} \right] \left[\lambda_3 \frac{Q(K_2^* - Q^*)}{|\mathbf{k}_2 - \mathbf{q}|} - \lambda_2 \frac{Q^* K_2}{k_2} \right] \quad (4.6)$$

Notice that the scattering amplitude, T , is singular for forward scattering: $T \sim 1/q$. This is a characteristic property of scattering between anyons [21]. We will have to keep careful track of this potential infrared singularity in our subsequent transport analysis.

Finally, we also express the electrical current, defined in (2.8), in terms of the γ_{\pm} . For the case of a spatially independent current (which is the only case of interest here), the result can be written as

$$\mathbf{J} = \mathbf{J}_I + \mathbf{J}_{II} \quad (4.7)$$

with

$$\mathbf{J}_I = qe \sum_{\lambda} \int \frac{d^2 k}{(2\pi)^2} \frac{\lambda \mathbf{k}}{k} \gamma_{\lambda}^\dagger(\mathbf{k}) \gamma_{\lambda}(\mathbf{k}) \quad (4.8)$$

and

$$\mathbf{J}_{II} = -iqe \int \frac{d^2 k}{(2\pi)^2} \frac{(\hat{\mathbf{z}} \times \mathbf{k})}{k} (\gamma_{+}^\dagger(\mathbf{k}) \gamma_{-}(\mathbf{k}) - \gamma_{-}^\dagger(\mathbf{k}) \gamma_{+}(\mathbf{k})) \quad (4.9)$$

where $\hat{\mathbf{z}}$, a unit vector orthogonal to the x, y plane. As in I, \mathbf{J}_I measures the current carried by motion of the quasiparticles and quasiholes—notice the λ prefactor, indicating that these excitations have opposite charges. The operator $\mathbf{J}_I I$ creates a quasiparticle-quasihole pair: throughout this section we will work in the approximation in which $\mathbf{J}_{II} = 0$. We will also neglect all mixing between the $\langle \gamma_{\pm}^\dagger \gamma_{\pm} \rangle$ and $\langle \gamma_{\pm}^\dagger \gamma_{\mp} \rangle$ distribution functions. These approximations simply amount to neglecting all but the $\tilde{\sigma}_{xx}^{\text{qp}}$ component of $\tilde{\sigma}$ —the other components were already computed satisfactorily in perturbation theory in Section III.

We can now use the standard equation of motion analysis [24] to write down the collisionless transport equations for the excitations. As a first step, we define the distribution functions

$$f_{\lambda}(\mathbf{k}, t) = \langle \gamma_{\lambda}^\dagger(\mathbf{k}, t) \gamma_{\lambda}(\mathbf{k}, t) \rangle. \quad (4.10)$$

In equilibrium in the absence of external perturbations, these are related to the Fermi function defined in (3.6)

$$\begin{aligned} f_+(\mathbf{k}, t) &= f^0(k) \\ f_-(\mathbf{k}, t) &= f^0(-k) = 1 - f^0(k) \end{aligned} \quad (4.11)$$

Then to first order in α , in the presence of an external electric field \mathbf{E} , we find the simple equations

$$\left(\frac{\partial}{\partial t} + qe\mathbf{E}_T \cdot \frac{\partial}{\partial \mathbf{k}} \right) f_\lambda(\mathbf{k}, t) = 0. \quad (4.12)$$

At this order, in the approximations discussed above, the only effect of the interactions has been to replace \mathbf{E} by \mathbf{E}_T . It is a simple matter to solve (4.12) in linear response. First we parametrize the change in f_λ from its equilibrium value by

$$f_\lambda(\mathbf{k}, \omega) = 2\pi\delta(\omega)f^0(\lambda k) + \lambda qe\mathbf{k} \cdot \mathbf{E}_T(\omega)g(k, \omega), \quad (4.13)$$

where we have performed a Fourier transform in time to frequencies, ω , and introduced the unknown function $g(k, \omega)$. Notice that the change in the distribution functions has an opposite sign for quasiparticles and quasiholes. Thus the quasiparticles and quasiholes move in opposite directions: as they have opposite charges, their electrical currents are equal, while their net momenta have opposite signs. Inserting (4.13) into (4.12), we can obtain a simple solution for the function g

$$g(k, \omega) = \frac{1}{(-i\omega + \eta)k} \left(-\frac{\partial f^0(k)}{\partial k} \right). \quad (4.14)$$

Inserting this result into (4.10) and (4.8), we obtain the conductivity

$$\tilde{\sigma}_{xx}^{\text{qp}}(\omega) = 2 \frac{2\pi q^2 e^2}{(-i\omega + \eta)h} \int \frac{d^2 k}{(2\pi)^2} \frac{k_x^2}{k^2} \left(-\frac{\partial f^0(k)}{\partial k} \right), \quad (4.15)$$

which is precisely our earlier result (3.13), in the approximation $M(T) = 0$ and $\mathcal{N}(\alpha) = \ln(2)$. In this approach, it is now evident that the leading factor of 2 comes from the sum over λ : *i.e.* the quasiparticles and quasiholes contribute equally to the total current.

B. Collision-dominated transport

We now include collision terms on the right hand side of (4.12). As in I, while the terms can be formally derived using the methods of Ref [24], it is easier to determine by a simple application of Fermi's golden rule. In the latter manner we obtained

$$\begin{aligned} & \left(\frac{\partial}{\partial t} + qe\mathbf{E}_T \cdot \frac{\partial}{\partial \mathbf{k}} \right) f_\lambda(\mathbf{k}, t) = \\ & - \int \frac{d^2 k_1}{(2\pi)^2} \frac{d^2 q}{(2\pi)^2} (2\pi)\delta(k + k_1 - |\mathbf{k} + \mathbf{q}| - |\mathbf{k}_1 - \mathbf{q}|) \left\{ \right. \\ & \left. |T_1|^2 \left\{ f_\lambda(\mathbf{k}, t) f_{-\lambda}(-\mathbf{k}_1 + \mathbf{q}, t) [1 - f_\lambda(\mathbf{k} + \mathbf{q}, t)] [1 - f_{-\lambda}(-\mathbf{k}_1, t)] \right. \right. \end{aligned}$$

$$\begin{aligned}
& - [1 - f_\lambda(\mathbf{k}, t)][1 - f_{-\lambda}(-\mathbf{k}_1 + \mathbf{q}, t)]f_\lambda(\mathbf{k} + \mathbf{q}, t)f_{-\lambda}(-\mathbf{k}_1, t) \} \\
& + \frac{1}{2} |T_2|^2 \left\{ f_\lambda(\mathbf{k}, t)f_\lambda(\mathbf{k}_1, t)[1 - f_\lambda(\mathbf{k} + \mathbf{q}, t)][1 - f_\lambda(\mathbf{k}_1 - \mathbf{q}, t)] \right. \\
& \left. - [1 - f_\lambda(\mathbf{k}, t)][1 - f_\lambda(\mathbf{k}_1, t)]f_\lambda(\mathbf{k} + \mathbf{q}, t)f_\lambda(\mathbf{k}_1 - \mathbf{q}, t) \right\}. \quad (4.16)
\end{aligned}$$

where

$$\begin{aligned}
T_1 & \equiv T_{+--+}(\mathbf{k}, -\mathbf{k}_1 + \mathbf{q}, \mathbf{q}) - T_{-+-+}(-\mathbf{k}_1 + \mathbf{q}, \mathbf{k}, \mathbf{k} + \mathbf{k}_1) \\
& \quad - T_{+-+-}(\mathbf{k}, -\mathbf{k}_1 + \mathbf{q}, -\mathbf{k} - \mathbf{k}_1) + T_{-++-}(-\mathbf{k}_1 + \mathbf{q}, \mathbf{k}, -\mathbf{q}) \\
T_2(\mathbf{k}, \mathbf{k}_1, \mathbf{q}) & \equiv T_{++++}(\mathbf{k}, \mathbf{k}_1, \mathbf{q}) - T_{++++}(\mathbf{k}_1, \mathbf{k}, \mathbf{k} + \mathbf{q} - \mathbf{k}_1) \\
& \quad - T_{++++}(\mathbf{k}, \mathbf{k}_1, \mathbf{k}_1 - \mathbf{k} - \mathbf{q}) + T_{++++}(\mathbf{k}_1, \mathbf{k}, -\mathbf{q}) \quad (4.17)
\end{aligned}$$

The terms proportional to $|T_1|^2$ represent collisions between oppositely charged particles, while those proportional to $|T_2|^2$ are collisions between like charges. There are also processes a particle-hole pair is created: as in I, these can be dropped because they have vanishing phase space upon imposition of the energy conservation constraint with dispersion $\varepsilon_k = k$

We now proceed to the linearization of (4.16) by inserting the parametrization (4.13) and find

$$\begin{aligned}
-i\omega kg(k, \omega) + \frac{\partial f^0(k)}{\partial k} = & \\
& - \int \frac{d^2 k_1}{(2\pi)^2} \frac{d^2 q}{(2\pi)^2} (2\pi) \delta(k + k_1 - |\mathbf{k} + \mathbf{q}| - |\mathbf{k}_1 - \mathbf{q}|) \left\{ \right. \\
& \left(\frac{(e^{(|\mathbf{k}_1 - \mathbf{q}| + |\mathbf{k} + \mathbf{q}|)/T} + e^{k_1/T})(|T_1|^2 + |T_2|^2/2)}{(e^{k_1/T} + 1)(e^{|\mathbf{k}_1 - \mathbf{q}|/T} + 1)(e^{|\mathbf{k} + \mathbf{q}|/T} + 1)} \right) kg(k, \omega) \\
& - \left(\frac{(e^{(|\mathbf{k}_1 - \mathbf{q}| + |\mathbf{k} + \mathbf{q}|)/T} + e^{k/T})(|T_1|^2 - |T_2|^2/2)}{(e^{k/T} + 1)(e^{|\mathbf{k}_1 - \mathbf{q}|/T} + 1)(e^{|\mathbf{k} + \mathbf{q}|/T} + 1)} \right) \left(\frac{\mathbf{k} \cdot \mathbf{k}_1}{k} \right) g(k_1, \omega) \\
& + \left(\frac{(e^{|\mathbf{k} + \mathbf{q}|/T} + e^{(k+k_1)/T})(|T_1|^2 - |T_2|^2/2)}{(e^{k/T} + 1)(e^{k_1/T} + 1)(e^{|\mathbf{k} + \mathbf{q}|/T} + 1)} \right) \left(\frac{\mathbf{k} \cdot (\mathbf{k}_1 - \mathbf{q})}{k} \right) g(|\mathbf{k}_1 - \mathbf{q}|, \omega) \\
& \left. - \left(\frac{(e^{|\mathbf{k}_1 - \mathbf{q}|/T} + e^{(k+k_1)/T})(|T_1|^2 + |T_2|^2/2)}{(e^{k/T} + 1)(e^{k_1/T} + 1)(e^{|\mathbf{k}_1 - \mathbf{q}|/T} + 1)} \right) \left(\frac{\mathbf{k} \cdot (\mathbf{k} + \mathbf{q})}{k} \right) g(|\mathbf{k} + \mathbf{q}|, \omega) \right\}. \quad (4.18)
\end{aligned}$$

The final ingredient necessary before assembling all the results of this paper is now a solution of (4.18) for the distribution function $g(k, \omega)$. An analytic solution is clearly out of the question and, we obtained the solution numerically. However, before attempting any numerical solution, the singular nature of the scattering cross-sections $|T_1|^2$ and $|T_2|^2$ makes it essential to obtain an analytic understanding of the nature of any potential infrared divergences arising from the momentum integration. We will show below that all the potentially infrared divergent terms in the collision integral do indeed vanish. However just this knowledge is not sufficient to allow one to proceed with the numerical integration. One does not want numerically integrate an integrand with potentially divergent terms which will eventually average out to a finite answer, as such a procedure is clearly prone to large systematic numerical errors; rather one wants an integrand which is explicitly free of singularities. On the

other hand, the integrand is dependent upon the unknown function g , so explicitly removing the singularities is difficult. These issues are clearly crucial, but also vexing, and stymied the author for some time. Eventually, a remarkably simple and useful parametrization of the collision term was found. As the analytic discussion of the cancellation of singularities is also simplest in this new parametrization, we will first introduce it, and then discuss the cancellation.

The key is to carry out the \mathbf{q} integration in the collision term of (4.18) first, and to notice that the delta function associated with energy conservation

$$\delta(k + k_1 - |\mathbf{k} + \mathbf{q}| - |\mathbf{k}_1 - \mathbf{q}|) \quad (4.19)$$

defines an ellipse in the \mathbf{q} plane with foci at $-\mathbf{k}$ and \mathbf{k}_1 . It therefore pays to parametrize \mathbf{q} in an *elliptic* co-ordinate system [25]. We introduce elliptic co-ordinates

$$0 \leq \mu < \infty \quad , \quad -\pi < \theta \leq \pi \quad (4.20)$$

and express \mathbf{q} in terms of μ and θ by

$$Q = \frac{K_1 - K}{2} + \frac{(K_1 + K)}{4} (e^{\mu+i\theta} + e^{-\mu-i\theta}). \quad (4.21)$$

Here \mathbf{k} and \mathbf{k}_1 are regarded as fixed external parameters, and \mathbf{k}_1 will be subsequently integrated over. Then it can be easily verified that the ellipse represented by (4.19) is given simply by

$$\cosh \mu = \frac{k + k_1}{|\mathbf{k} + \mathbf{k}_1|} \quad (4.22)$$

The integral over \mathbf{q} in (4.18) is a two-dimensional integral over μ and θ , and the integral over μ can now be trivially carried out. This is summarized by the general formula

$$\begin{aligned} \int \frac{d^2 q}{(2\pi)^2} (2\pi) \delta(k + k_1 - |\mathbf{k} + \mathbf{q}| - |\mathbf{k}_1 - \mathbf{q}|) F(\mathbf{q}, \mathbf{k}, \mathbf{k}_1) \\ = \int_0^{2\pi} \frac{d\theta}{2\pi} \int_0^\infty d\mu \frac{|\mathbf{k} + \mathbf{k}_1|^2}{4} (\cosh^2 \mu - \cos^2 \theta) \delta(k + k_1 - |\mathbf{k} + \mathbf{k}_1| \cosh \mu) F(Q, K, K_1) \\ = \int_0^{2\pi} \frac{d\theta}{2\pi} \frac{|\mathbf{k} + \mathbf{k}_1| (\cosh^2 \mu - \cos^2 \theta)}{4 \sinh \mu} F(Q, K, K_1), \end{aligned} \quad (4.23)$$

where F is an arbitrary function, and in the last equation we use the value of μ given in (4.22) and Q given in (4.21).

We are now prepared to discuss the handling of the infrared divergences in (4.18). There are two distinct types of potential divergences and we will consider them in turn.

- The first singularity is associated with the divergence in the forward scattering cross-section. By an examination of (4.17) we see that there is a $1/q^2$ divergence in $|T_1|^2$ when the momentum transfer \mathbf{q} approaches zero, and also a $1/(\mathbf{q} - \mathbf{k}_1 + \mathbf{k})^2$ divergence in $|T_2|^2$ when the momentum transfer \mathbf{q} approaches $\mathbf{q} = \mathbf{k}_1 - \mathbf{k}$; the latter divergence

corresponds to forward scattering with an exchange of particles. (Note that there is no divergence when the momentum transfer $\mathbf{k} + \mathbf{k}_1$ vanishes, as is easily seen by an examination of the λ labels in (4.17), combined with the expression (4.6)). However, we then notice from the right hand side of (4.18) that the coefficient of $|T_1|^2$ in the collision term vanishes at $\mathbf{q} = 0$; the term in the co-efficient linear in \mathbf{q} will vanish after an appropriate angular integral over \mathbf{q} , and the remaining combination is explicitly finite at $\mathbf{q} = 0$. Similar considerations apply to the the coefficient of $|T_2|^2$, which vanishes at $\mathbf{q} = \mathbf{k}_1 - \mathbf{k}$. The physics of this cancellation is simple and quite familiar. Its origin is the “ $(1 - \cos(\text{scattering angle}))$ ” phase space factor that appears in the expression for transport relaxation rates [26]: this vanishes at zero scattering angle, and cancels out the divergence in the scattering cross-section.

Now there remains the issue of how to numerically treat this potential divergence. It is clear that the angular integral around $\mathbf{q} = 0$ and $\mathbf{q} = \mathbf{k}_1 - \mathbf{k}$ should be taken with great care, or we will be left with a spurious divergence. Here our elliptical parametrization (4.21) turns out to be helpful. Notice that, as must be the case, the points $\mathbf{q} = 0$ and $\mathbf{q} = \mathbf{k}_1 - \mathbf{k}$ satisfy the delta function in (4.19), and therefore lie on the ellipse defined by (4.22). These points lie at $\theta = \theta_0$ and $\theta = \theta_0 + \pi$ where θ_0 is determined by the equation

$$2 \frac{K - K_1}{K + K_1} = e^{\mu+i\theta_0} + e^{-\mu-i\theta_0} \quad (4.24)$$

This is a quadratic equation for $e^{i\theta_0}$, and therefore has two solutions which are easily determined. For μ give by (4.22), one of the solution will have unit modulus and therefore determines a real θ_0 : this is guaranteed by the fact that $\mathbf{q} = 0$ lies on the ellipse defined by (4.22). The angular averaging is carried out by the θ integral in (4.23), and we now simply have to insure that the vicinities of the points $\theta = \theta_0$ (and $\theta = \theta_0 + \pi$) are treated symmetrically. More precisely, we always pair the integrands at $\theta_0 + \theta$ and $\theta_0 - \theta$ (and also at $\theta_0 + \pi + \theta$ and $\theta_0 + \pi - \theta$) so that the combined integrand is explicitly finite at the potentially singular points.

- The second potential singularity arises purely from phase space considerations, and is a curious property of energy-conserving scattering of particles in two dimensions with the linear dispersion $\varepsilon_k = k$. We are considering the scattering of two incoming particles with momenta \mathbf{k} and \mathbf{k}_1 . Consider the case where these two momenta are collinear and point in the same direction *i.e.* when $\mathbf{k} \cdot \mathbf{k}_1 = kk_1$. We are eventually integrating over \mathbf{k}_1 in the collision term of (4.18), and this condition defines a semi-infinite line in the two-dimensional \mathbf{k}_1 space. Along this line, we see from (4.22) that $\mu = 0$. Now the phase space factor $1/\sinh \mu$ in (4.23) looks dangerous (generically the \mathbf{q} integral in (4.23) will be non-singular, and will not effect the considerations here). This infinite factor is present along the entire semi-infinite line in the \mathbf{k}_1 plane: if we pick a point a distance y from this line (almost collinear particles) we find that the $1/\sinh \mu$ factor diverges as $1/y$. This implies a logarithmic divergence in the \mathbf{k}_1 integral. Fortunately, the specific form of T_1, T_2 under consideration here comes to the rescue. It is easy to show from (4.6,4.17) that these cross-sections vanish identically for the case of the scattering of particles moving in the same direction.

The remaining steps in the solution of the integral equation were relatively straightforward. It is easy to show that $g(k, \omega) \sim e^{-k/T}$ for large k , and so it is an excellent approximation to simply truncate the infinite range of k integration at some large positive k . Over this finite range, we expanded $g(k, \omega)e^{k/T}$ over the space of Chebyshev polynomials. We determined the action of the kernel of the integral equation on each Chebyshev polynomials, and decomposed the resultant also over Chebyshev polynomials. This defined a discrete matrix, which is the transcription of the kernel to the discrete basis space of Chebyshev polynomials. Solving the integral equation then simply became a matter of inverting the matrix. Notice that as the kernel does not explicitly depend upon frequency, the same matrix could be used at any frequency.

We now present the results of the above numerical analysis. A simple dimensional analysis of (4.18) shows that the entire T and α dependence of the integral equation can be scaled out, and the resulting scaled equation is parameter free. In particular the solution of (4.18) has the form

$$g(k, \omega) = \frac{1}{\alpha^2 T^3} G\left(\frac{k}{T}, \frac{\omega}{\alpha^2 T}\right), \quad (4.25)$$

where G is a universal function we have determined numerically. Inserting the form (4.25) into (4.13) and (4.8) we see that the conductivity (3.13,4.15) is now replaced by

$$\tilde{\sigma}_{xx}^{\text{qp}}(\omega) = \frac{q^2 e^2}{\alpha^2 h} \tilde{\Sigma}_{xx}^{\text{qp}}\left(\frac{\omega}{\alpha^2 T}\right) \quad (4.26)$$

with the universal scaling function $\tilde{\Sigma}_{xx}^{\text{qp}}$ given by

$$\tilde{\Sigma}_{xx}^{\text{qp}}(\tilde{\omega}) = \int_0^\infty \bar{k}^2 d\bar{k} G(\bar{k}, \tilde{\omega}) \quad (4.27)$$

This scaling function describes the broadening of the delta function in the real part of (4.15): the large frequency behavior of (4.18) shows that it has the same total spectral weight as (4.15):

$$\int_0^\infty \frac{d\tilde{\omega}}{\pi} \text{Re} [\tilde{\Sigma}_{xx}^{\text{qp}}(\tilde{\omega})] = \frac{\ln(2)}{2} \quad (4.28)$$

We show the numerical solutions for the universal functions G and $\tilde{\Sigma}_{xx}^{\text{qp}}$ in Figs 3 and 4 respectively. The value of $\tilde{\Sigma}_{xx}^{\text{qp}}(0)$ determines the d.c. conductivity

$$\tilde{\sigma}_{xx}(\omega/T \rightarrow 0) = \left(\frac{q^2 e^2}{h}\right) \frac{0.437}{\alpha^2} \quad (4.29)$$

This result and (3.17) and (3.28) completely specify the limiting forms of the conductivity $\tilde{\sigma}$.

V. SYNTHESIS

We will now finally turn to a discussion of the properties of the physical conductivity σ . The several disparate ingredients necessary for its computation have all been assembled, and let us now summarize them. We began with a model with two species of anyons $\psi_{1,2}$. We defined their irreducible conductivities $\tilde{\sigma}_{1,2}$ and argued that the physical conductivity σ was related to them by (2.13). The ψ_2 anyons were non-critical and the value of $\tilde{\sigma}_2$ is given simply by (2.14). Sections III and IV were devoted to studying the value of the critical $\tilde{\sigma}_1$. Section III considered the perturbative contribution which in the limit $\omega/T \rightarrow \infty$ reduced to the coherent transport of externally created particle-hole pairs. The Hall conductivity was given entirely by such a contribution: $\tilde{\sigma}_{xy}^{(1)} + \tilde{\sigma}_{xy}^{(2)} + \tilde{\sigma}_{xy}^{(3)}$ where the results are given in (3.19), (3.23) and (3.24) respectively. The longitudinal conductivity consists of the coherent contribution $\tilde{\sigma}_{xx}^{\text{coh}}$ given in (3.15), and an incoherent quasiparticle contribution $\tilde{\sigma}_{xx}^{\text{qp}}$ which was computed in Section IV; the latter satisfies the scaling form (4.26) and the scaling function $\tilde{\Sigma}_{xx}^{\text{qp}}$ was plotted in Fig 4.

The above discussion can be restated as follows. Let us define the dimensionless functions A, B by

$$\begin{aligned} A(\omega) &= \frac{h}{q^2 e^2} \left(\tilde{\sigma}_{xx}^{\text{qp}}(\omega) + \tilde{\sigma}_{xx}^{\text{coh}}(\omega) \right) \\ B(\omega) &= -\frac{1}{2} + \frac{h}{q^2 e^2} \left(\tilde{\sigma}_{xy}^{(1)}(\omega) + \tilde{\sigma}_{xy}^{(2)}(\omega) + \tilde{\sigma}_{xy}^{(3)}(\omega) \right) \end{aligned} \quad (5.1)$$

Then, the physical conductivities are given by

$$\begin{aligned} \sigma_{xx}(\omega) &= \left(\frac{q^2 e^2}{h} \right) \frac{A(\omega)}{\alpha^2 A^2(\omega) + (1 + \alpha B(\omega))^2} \\ \sigma_{xy}(\omega) &= \left(\frac{q^2 e^2}{h} \right) \frac{B(\omega) + \alpha(A^2(\omega) + B^2(\omega))}{\alpha^2 A^2(\omega) + (1 + \alpha B(\omega))^2} \end{aligned} \quad (5.2)$$

We emphasize that A and B are complex, universal functions of ω/T , and it is necessary to include both their real and imaginary parts in the above expressions.

In evaluating our final results for σ_{xx} , an important complicating factor becomes apparent. While we are ultimately interested in α of order unity, the terms entering (5.2) are of many differing orders in α for small α . As a result, certain processes become unphysically dominant at small α , while in the real system we expect a more even-handed competition. Further the terms also vary on differing scales of ω . In particular, the quasiparticle/quasihole conductivity $\tilde{\sigma}_{xx}^{\text{qp}}$ is of overall order $1/\alpha^2$ and varies on a frequency scale $\omega \sim \alpha^2 T$; for small ω it is the most dominant term as $\alpha \rightarrow 0$. Of the other terms, $\tilde{\sigma}_{xx}^{\text{coh}}$ is order unity, while $\tilde{\sigma}_{xy}^{(1,2,3)}$ are of order α , and all vary on a scale $\omega \sim T$; these become important for large ω as $\alpha \rightarrow 0$. Because of these complications, we believe more significance should be attached to the form of our results for the individual conductivities in Section III and IV. The final results, when these distinct components are combined, are expected to be less reliable for moderate α .

We begin by describing the formal structure of the small α expansion for σ . It is necessary to consider two distinct frequency regimes separately:

(A) ω of order $\alpha^2 T$, but with $\omega \ll T$: In this σ_{xx}^{qp} is the dominant term, and examination of the small α limit of (5.2) gives

$$\sigma_{xx}(\omega) = \left(\frac{q^2 e^2}{h}\right) \left[\frac{1}{\tilde{\Sigma}_{xx}^{\text{qp}}(\omega/\alpha^2 T)} + \dots \right] \quad (5.3)$$

We show a plot of the result above for $\text{Re}[\sigma_{xx}(\omega)]$ in Fig 5. Notice that this is not simply the inverse of the real plot in Fig 4, as the first equation in (5.3) involves the inverse of the *complex* function $\tilde{\Sigma}_{xx}^{\text{qp}}$. The function $\text{Re}[1/\tilde{\Sigma}_{xx}^{\text{qp}}(\tilde{\omega})]$ approaches a finite number in both the limits $\tilde{\omega} \rightarrow 0$ (where it is simply the inverse of (4.29)) and $\tilde{\omega} \rightarrow \infty$:

$$\begin{aligned} \text{Re} \left[\frac{1}{\tilde{\Sigma}_{xx}^{\text{qp}}(\tilde{\omega} \rightarrow 0)} \right] &= 2.29 \\ \text{Re} \left[\frac{1}{\tilde{\Sigma}_{xx}^{\text{qp}}(\tilde{\omega} \rightarrow \infty)} \right] &= 3.47 \end{aligned} \quad (5.4)$$

In a similar manner, we can also get the Hall conductivity in this regime:

$$\sigma_{xy}(\omega) = \left(\frac{q^2 e^2}{h}\right) \left[\frac{1}{\alpha} + \dots \right] \quad (5.5)$$

Surprisingly, this result for σ_{xy} has the opposite sign from the Hall conductivity of the quantized Hall phase connected to the critical point under consideration here: we strongly suspect this feature is an artifact of the absence scattering from interactions other than the Chern Simons term: a model in which $\tilde{\sigma}_{xx}^{\text{qp}}$ is not so singular in the small α limit should have a Hall conductivity of the “correct” sign.

(B) ω of order or larger than T : Now the result is constructed simply by inserting the perturbative results of Section III for $\tilde{\sigma}$ in (5.2). The formal small α expansion is

$$\begin{aligned} \sigma_{xx}(\omega) &= (1 + \alpha) \tilde{\sigma}_{xx}^{\text{coh}}(\omega) \\ \sigma_{xy}(\omega) &= -\frac{q^2 e^2}{2h} + \tilde{\sigma}_{xy} + \left[-\frac{q^2 e^2}{4h} + \frac{h}{q^2 e^2} \{\tilde{\sigma}_{xx}^{\text{coh}}(\omega)\}^2 \right] \alpha + \dots, \end{aligned} \quad (5.6)$$

and the ingredients determining the coefficients were plotted in Figs 1 and 2.

An alternative approach to gaining some understanding of the predictions of (5.2) is to simply evaluate the full expression at a given value of α . This has been done in Figs 6 and 7, which show the results of directly evaluating (5.2) at face value at $\alpha = 0.3$.

VI. CONCLUSIONS

The purpose of this paper was to describe the dynamic transport properties of the the simplest possible quantum critical point in a quantum Hall system. In particular, motivated by experimental results discussed in Section I, we chose a model quantum phase transition which had non-zero interactions in the critical fixed point theory. The critical properties of such theories have a *universal* dependence of all observables on ω/T , and, as pointed in I,

the dependence of the conductivity on ω/T at two dimensional quantum critical points is especially important. The model we chose, \mathcal{S} in (2.1), is equivalent to a model of free anyons and anti-anyons with a relativistic Dirac spectrum. This model is properly considered as an interacting theory for the following reason: two anyonic/anti-anyonic excitations have a non-trivial T matrix for scattering [21] in which the momenta of the ingoing and outgoing particles can be arbitrary, and are subject only to the constraints of conservation of total energy and momentum (it is clear that this fails only for purely bosonic or fermionic statistics, when the ingoing and outgoing momenta are the same). Such scattering is the main ingredient in establishing local equilibrium, and is essential to the description of transport in the regime $\omega \ll T$.

Our results for the non-zero temperature transport properties were summarized in Section V. It is evident from the discussion there that, while the general scaling forms for the conductivities are very similar to those discussed in I for the boson superfluid-insulator transition, the explicit results for the scaling functions themselves are quite different. For instance, we found in I that the longitudinal conductivity $\sigma_{xx}(\omega)$ was a decreasing function of increasing ω near $\omega = 0$. In the present quantum Hall problem, we found that for small α , the longitudinal conductivity satisfied (5.3), and is therefore seen to be an increasing function of ω near $\omega = 0$, as shown in Fig 5. This property was subsequently responsible for a peak in σ_{xx} near $\omega \sim T$ shown in Fig 6.

As they stand, our model calculations can probably not be directly applied to microwave conductivity measurements in the quantum Hall system [14]. The most important defect that must be repaired is the absence of Coulomb interactions among the charged excitations. A simple power counting argument shows that the Coulomb interaction is a marginal perturbation at the fixed point considered here. A theory for the consequences of this marginal perturbation is not available at present, and appears to us to be an important subject for future research. It is interesting to note that since the Coulomb interaction is marginal at tree level, it must be characterized by a dimensionless coupling constant. It is easy to see that this coupling constant is

$$\frac{e^2}{\hbar v} = \left(\frac{e^2}{\hbar c} \right) \frac{c}{v} \approx \frac{c/v}{137} \quad (6.1)$$

where v is the velocity of the Dirac fermions, c is the velocity of light, and the quantity in the parenthesis is the dimensionless fine structure constant. For v , it seems reasonable to use a typical drift velocity of electrons in the two-dimensional electron gas $\sim 10^4 - 10^5 m/s$, and we see then that this dimensionless coupling can be quite large. The Dirac fermion model (at $\alpha = 0$) also describes quasiparticles in a d-wave superconductor, and so the dimensionless coupling characterizing the Coulomb interactions can also be quite large for the high temperature superconductors.

ACKNOWLEDGMENTS

I am grateful to K. Damle, S. Girvin, N. Read, R. Shankar, S. Sondhi, Y.-S. Wu, and J. Ye for helpful discussions. This research was supported by the National Science Foundation Grant No. DMR-96-23181.

APPENDIX A: LARGE N EXPANSION

Our study of transport near the superfluid-insulator quantum critical point in I, and of the quantum Hall critical point in the present paper, has been carried out using transport equations in which a four-point coupling between the charge carriers is used as an expansion parameter. In this appendix we will outline an alternative approach to the same problems, the large N expansion. We shall not provide an explicit numerical solution of the large N transport equations here, but it will be evident that the structure of the results is very similar to those already obtained.

We will begin with the simpler case of the superfluid-insulator transition in a model of $O(2)$ quantum rotors which was discussed in I. We generalize this to a model of $O(N)$ quantum rotors, and the quantum field theory describing the critical point has the action

$$\mathcal{S}_r = \int_0^{1/T} d\tau \int d^2x \left\{ \frac{1}{2} \left[(\partial_\tau \phi_a)^2 + c^2 (\nabla_x \phi_a)^2 + m_{0c}^2 \phi_a^2 \right] + \frac{u_0}{2N} (\phi_a^2)^2 \right\}. \quad (\text{A1})$$

Here ϕ_a is a N -component field and the action has $O(N)$ symmetry (the $O(N)$ index a is implicitly summed over). The spatial and temporal gradient terms are both second order, so the action has a “Lorentz” invariance with c the velocity of light, and as a result the dynamic critical exponent $z = 1$; we will henceforth use units in which $c = 1$. The quartic non-linearity, u_0 , has been scaled by a factor of $1/N$ to allow the interesting large N limit. The bare “mass” term, m_{0c}^2 , is cutoff dependent, and must be adjusted order by order in u_0 so that the system is at its quantum critical point at $T = 0$. The superfluid-insulator transition of boson Hubbard models is described by the case $N = 2$, where $\Psi = \phi_1 + i\phi_2$ is the usual complex superfluid order parameter. The case $N = 3$ which applies to quantum-critical points in quantum antiferromagnets [22,27].

First we review the large $1/N$ expansion for the order parameter susceptibility, which is the propagator, G , of the ϕ_a field. This was extensively discussed in Ref [27]. At momentum \mathbf{k} , and Matsubara frequency ω_n , the $N = \infty$ result for this propagator is

$$G(\mathbf{k}, i\omega_n) = \frac{1}{\omega_n^2 + k^2 + \Theta^2 T^2}, \quad (\text{A2})$$

where Θ is a pure (universal) number:

$$\Theta = 2 \ln \left(\frac{\sqrt{5} + 1}{2} \right) \quad (\text{A3})$$

The $1/N$ corrections are obtained by decoupling the quartic term in (A1) by a Hubbard-Stratanovich field $\tilde{\lambda}$ (not to be confused with the charge subscript λ used in Section IV, and also below). There is then a three-point coupling $\sim \phi_a^2 \tilde{\lambda}$ in the action. The propagator of the $\tilde{\lambda}$ field is given by the inverse of the bubble graph of the ϕ_a field. In the low-energy, long-distance limit relevant for the critical properties, this propagator becomes independent of the microscopic value of u_0 , and equals

$$\frac{2}{N} \frac{1}{\Pi(\mathbf{q}, i\epsilon_n)} \quad (\text{A4})$$

where

$$\Pi(\mathbf{q}, i\epsilon_n) = T \sum_{\omega_n} \int \frac{d^2 k}{(2\pi)^2} G(\mathbf{k}, i\omega_n) G(\mathbf{k} + \mathbf{q}, i\omega_n + i\epsilon_n) \quad (\text{A5})$$

Notice that there is a factor of $1/N$ associated with each $\tilde{\lambda}$ propagator: this comes from the sum over the N components of the ϕ_a field in the bubble graph. So the $1/N$ expansion for the susceptibility is generated by expanding in the number of $\tilde{\lambda}$ propagators.

Now we turn to transport properties. The value of the conductivity at $N = \infty$ was discussed in Section II of I. The structure was very similar to that obtained in an expansion in $\epsilon = 3 - d$: there was a quasiparticle/quasihole delta function at $\omega = 0$, and a continuum contribution at frequencies greater than $\omega = 2\Theta T$. The main purpose of this appendix is to determine the manner in which the $\omega = 0$ delta function broadens out in the $1/N$ expansion. Naturally, this will be done by formulating the transport equations of the quasiparticles and quasiholes in the large N limit.

The general N transport equations for \mathcal{S}_r were discussed in Appendix B of I in an expansion in u_0 . Following that treatment, we consider here the linear response to an “electric” field, \mathbf{E} , which couples only to the $\phi_{1,2}$ components *i.e.* the corresponding electric potential couples to a generator of $O(N)$ which rotates the system in the 1, 2 plane. Then it was argued that the distribution function of excitations in the remaining components remained unchanged to linear order in the field—all corrections are at least quadratic in \mathbf{E} . In other words, if, as in I, we make the mode expansion in terms of particle creation and annihilation operators

$$\phi_a(\mathbf{x}, t) = \int \frac{d^2 k}{(2\pi)^2} \frac{1}{\sqrt{2\varepsilon_k}} \left(b_a(\mathbf{k}, t) e^{i\mathbf{k}\cdot\mathbf{x}} + b_a^\dagger(\mathbf{k}, t) e^{-i\mathbf{k}\cdot\mathbf{x}} \right), \quad (\text{A6})$$

with the dispersion

$$\varepsilon_k = (k^2 + \Theta^2 T^2)^{1/2}, \quad (\text{A7})$$

then, we have

$$f_a(\mathbf{k}, t) \equiv \langle b_a^\dagger(\mathbf{k}, t) b_a(\mathbf{k}, t) \rangle = n(\varepsilon_k) \equiv \frac{1}{e^{\varepsilon_k/T} - 1} \quad \text{for } a > 2. \quad (\text{A8})$$

This has very important consequences for the large N expansion. Recall that the inverse propagator of the $\tilde{\lambda}$ field was given by the sum over the bubble graphs of the N components of the ϕ_a . In the large N limit, this sum is dominated by the $a > 2$ components, and so also remains unaffected to linear order in \mathbf{E} . So we can assume that the propagator for $\tilde{\lambda}$ is still given by (A4).

Now the quantum transport equations can be easily written down by noticing that the present problem has a structure closely analogous to the electron-phonon problem [26,28]: the $\tilde{\lambda}$ field plays a role similar to the phonons, and the $\phi_a^2 \tilde{\lambda}$ coupling is analogous to the electron-phonon coupling. The fact that the $\tilde{\lambda}$ propagator is not modified by \mathbf{E} is equivalent to the statement that “phonon drag” effects are negligible in the large N limit. Indeed, the particular form of the propagator in (A4) translates into a special phonon density of states, and the transport equations can then be read directly off Ref [28]. Let us define

$$b_{\pm}(\mathbf{k}, t) \equiv \frac{b_1(\mathbf{k}, t) \pm b_2(\mathbf{k}, t)}{\sqrt{2}}. \quad (\text{A9})$$

Then $f_{\lambda}(\mathbf{k}, t) = \langle b_{\lambda}^{\dagger}(\mathbf{k}, t) b_{\lambda}(\mathbf{k}, t) \rangle$, with $\lambda = \pm$ satisfies the transport equation

$$\begin{aligned} \left(\frac{\partial}{\partial t} + \lambda Q \mathbf{E} \cdot \frac{\partial}{\partial \mathbf{k}} \right) f_{\lambda}(\mathbf{k}, t) = & -\frac{2}{N} \int_0^{\infty} \frac{d\Omega}{\pi} \int \frac{d^2 q}{(2\pi)^2} \text{Im} \left(\frac{1}{\Pi(\mathbf{q}, \Omega)} \right) \\ & \times \left\{ \frac{(2\pi)\delta(\varepsilon_k - \varepsilon_{|\mathbf{k}+\mathbf{q}|} - \Omega)}{4\varepsilon_k \varepsilon_{|\mathbf{k}+\mathbf{q}|}} \left[f_{\lambda}(\mathbf{k}, t)(1 + f_{\lambda}(\mathbf{k} + \mathbf{q}, t))(1 + n(\Omega)) \right. \right. \\ & \quad \left. \left. - f_{\lambda}(\mathbf{k} + \mathbf{q}, t)(1 + f_{\lambda}(\mathbf{k}, t))n(\Omega) \right] \right. \\ & + \frac{(2\pi)\delta(\varepsilon_k - \varepsilon_{|\mathbf{k}+\mathbf{q}|} + \Omega)}{4\varepsilon_k \varepsilon_{|\mathbf{k}+\mathbf{q}|}} \left[f_{\lambda}(\mathbf{k}, t)(1 + f_{\lambda}(\mathbf{k} + \mathbf{q}, t))n(\Omega) \right. \\ & \quad \left. \left. - f_{\lambda}(\mathbf{k} + \mathbf{q}, t)(1 + f_{\lambda}(\mathbf{k}, t))(1 + n(\Omega)) \right] \right. \\ & + \frac{(2\pi)\delta(\varepsilon_k + \varepsilon_{|-\mathbf{k}+\mathbf{q}|} - \Omega)}{4\varepsilon_k \varepsilon_{|-\mathbf{k}+\mathbf{q}|}} \left[f_{\lambda}(\mathbf{k}, t)f_{-\lambda}(-\mathbf{k} + \mathbf{q}, t)(1 + n(\Omega)) \right. \\ & \quad \left. \left. - (1 + f_{-\lambda}(-\mathbf{k} + \mathbf{q}, t))(1 + f_{\lambda}(\mathbf{k}, t))n(\Omega) \right] \right\}, \quad (\text{A10}) \end{aligned}$$

where Q is the charge of the b_a quanta. Now this equation can be linearized like (4.16), and then solved using the numerical methods discussed in Section IV. We will not present the numerical solution here, but an essential fact is already clear from the structure of (A10). The $\omega = 0$ delta function in the conductivity, found at $N = \infty$, gets broadened out to a width $\omega \sim T/N$, and the peak conductivity at $\omega = 0$ is of order N .

The above large N analysis can obviously be carried out at any $1 < d < 3$. It is useful to do this and then take the limit of small $3 - d$. We find that the equation so obtained agrees *precisely* with the large N limit of the small $3 - d$ equation discussed in Appendix B of I for general N . Thus the $N \rightarrow \infty$ and $3 - d \rightarrow 0$ limits of the quantum transport equations commute, and this is an important check of the consistency of our analysis.

Our results can be easily extended to the large N limit of either bosonic [18] or fermionic [19] theories with Chern-Simons terms. For instance, an alternative formulation of the theory of anyons considered in this paper is to represent them as relativistic bosons with attached statistical flux tubes: this is represented by a generalization of the action \mathcal{S}_r as follows [18]. Consider the case with $N = 2M$ even, parametrize the $2N$ real fields ϕ_a in terms of M complex fields Ψ

$$\Psi_a = (\phi_{2a-1} + i\phi_{2a})/\sqrt{2} \quad a = 1 \dots M \quad (\text{A11})$$

Now couple a $U(1)$ Chern Simons field to the diagonal $U(1)$ charge

$$\begin{aligned} \mathcal{S}_{ra} = & \int_0^{1/T} d\tau \int d^2 x \left\{ |(\partial_{\tau} - ia_{\tau})\Psi_a|^2 + c^2 |(\nabla_x - ia_x)\Psi_a|^2 + m_{0c}^2 |\Psi_a|^2 \right. \\ & \left. + \frac{u_0}{M} (|\Psi_a|^2)^2 + \frac{iM}{4\pi\alpha} \epsilon_{\mu\nu\lambda} a_{\mu} \partial_{\nu} a_{\lambda} \right\}. \quad (\text{A12}) \end{aligned}$$

Notice that the effective statistics parameter of the anyons is α/M : this is necessarily very close of the bosonic limit for large M .

The large M analysis of \mathcal{S}_{ra} is very similar to that of \mathcal{S} : in addition to the field $\tilde{\lambda}$, we now have a gauge field a_μ whose propagator is also given by a boson current polarization bubble, and is of order $1/M$ [18]. By arguments very similar to those for $\tilde{\lambda}$, we can conclude that the deviations in the a_μ propagator due to the external electric field can be neglected *i.e.* “photon drag” is negligible in the large M limit. The resulting quantum transport equation is then very similar (A10): along with the terms already displayed, we have an additional parallel set with $\text{Im}(1/\Pi)$ replaced by the spectral density of the a_μ propagator times current matrix elements of the Ψ field.

Finally, similar considerations apply to the large M generalization of the fermionic Chern-Simons theory, \mathcal{S} , of this paper. We replicate the fermionic terms in \mathcal{S} M times, rescale $\alpha \rightarrow \alpha/M$, and then take the large M limit as discussed above for the bosonic theories.

APPENDIX B: COMPUTATIONS FOR THE HALL CONDUCTIVITY

This appendix shows how the result (3.20) is obtained from (3.19). First it is clear after using (3.7) and rescaling the integrand by T that

$$\tilde{\sigma}_{xy}^{(1)}(\omega/T \rightarrow 0) = \frac{q^2 e^2 \alpha}{h} \ln(2) \int_{2\alpha \ln(2)}^{\infty} \frac{d\varepsilon}{\varepsilon^2} \tanh(\varepsilon/2) \quad (\text{B1})$$

Let us define

$$F(y) = \int_y^{\infty} \frac{dx}{x^2} \tanh(x/2), \quad (\text{B2})$$

and it is clear that to understand the small α limit of (B1), we need the form of $F(y \rightarrow 0)$. By integrating twice by parts, it is easy to show that

$$F(y) = \frac{\tanh(y/2)}{y} - \frac{\ln(y/2)}{2 \cosh^2(y/2)} + \int_{y/2}^{\infty} dx \frac{\ln(x) \sinh(x)}{\cosh^3(x)} \quad (\text{B3})$$

Now we can explicitly take the $y \rightarrow 0$ limit to get

$$F(y \rightarrow 0) = \frac{1}{2} \ln(1/y) + \frac{\ln(2) + 1}{2} + \int_0^{\infty} dx \frac{\ln(x) \sinh(x)}{\cosh^3(x)} \quad (\text{B4})$$

Then, we evaluate the last integral by first expanding the integrand as an infinite series in e^{-2x} :

$$\begin{aligned} \int_0^{\infty} dx \frac{\ln(x) \sinh(x)}{\cosh^3(x)} &= -4 \int_0^{\infty} dx \ln(x) \left[\sum_{n=1}^{\infty} (-1)^n n^2 e^{-2nx} \right] \\ &= 2 \sum_{n=1}^{\infty} (-1)^n n (\gamma + \ln(2n)) \\ &= 2 \sum_{n=1}^{\infty} (-1)^n \left((\gamma + \ln(2)) n^{1+s} + \frac{d}{ds} n^{1+s} \right) \Big|_{s=0} \end{aligned}$$

$$\begin{aligned}
&= 6(\gamma + \ln(2))\zeta(-1) + 2 \frac{d}{ds} \left((2^{2+s} - 1)\zeta(-1-s) \right) \Big|_{s=0} \\
&= -\frac{\gamma}{2} - \frac{7\ln(2)}{6} - 6\zeta'(-1).
\end{aligned} \tag{B5}$$

Notice that the intermediate steps involve badly divergent series in n , and so the validity of the final result is not a priori obvious. To check it, we numerically evaluated the left hand side and verified that it was equal to the final right hand side to a very high accuracy. Combining (B1), (B2), (B4) and (B4), we can now obtain (3.20).

REFERENCES

- [1] *Perspectives in Quantum Hall Effects*, S. Das Sarma and A. Pinczuk eds, Wiley, New York (1997).
- [2] B. Hckenstein, Rev. Mod. Phys. **67**, 357 (1995).
- [3] S.L. Sondhi, S.M. Girvin, J.P. Carini and D. Shahar, Rev. Mod. Phys. **69**, 315 (1997).
- [4] S. Das Sarma in Chapter 1 of Ref [1].
- [5] A.M.M. Pruisken in *The Quantum Hall Effect*, R.E. Prange and S.M. Girvin eds, Springer-Verlag, New York (1990).
- [6] J.T. Chalker and P.D. Coddington, J. Phys. C **21**, 2665 (1988).
- [7] J.K. Jain, S. Kivelson and N. Trivedi, Phys. Rev. Lett. **64**, 1297 (1990).
- [8] S. Kivelson, D.H. Lee and S.C. Zhang, Phys. Rev. B **46**, 2223 (1992).
- [9] D.B. Chklovskii and P.A. Lee, Phys. Rev. B **48**, 18060 (1993).
- [10] D.G. Polyakov and B.I. Shklovskii, Phys. Rev. B **48**, 11167 (1993); D.G. Polyakov cond-mat/9608013; D.G. Polyakov and K.V. Samokhin, cond-mat/9705154.
- [11] K. Damle and S. Sachdev, Phys. Rev. B in press; cond-mat/9705206.
- [12] H.P. Wei, L.W. Engel and D.C. Tsui, Phys. Rev. B **50**, 14609 (1994).
- [13] M.P.A. Fisher, G. Grinstein, and S.M. Girvin, Phys. Rev. Lett. **64**, 587 (1990); M.P.A. Fisher, Phys. Rev. Lett. **65**, 923 (1990).
- [14] L.W. Engel, D. Shahar, C. Kurdak, and D.C. Tsui, Phys. Rev. Lett. **71**, 2638 (1993).
- [15] S. Sachdev, N. Read and R. Oppermann, Phys. Rev. B, **52**, 10286 (1995).
- [16] D.J. Thouless, M. Kohmoto, M.P. Nightingale and M. den Nijs, Phys. Rev. Lett. **49**, 405 (1982); Q. Niu, D.J. Thouless, and Yong-Shi Wu, Phys. Rev. B **31**, 3372 (1985).
- [17] A. Kol and N. Read, Phys. Rev. B **48**, 8890 (1993).
- [18] X.G. Wen and Yong-Shi Wu, Phys. Rev. Lett. **70**, 1501 (1993).
- [19] W. Chen, M.P.A. Fisher, and Yong-Shi Wu, Phys. Rev. B **48**, 13749 (1993).
- [20] D. Pfannkuche and A.H. MacDonald, cond-mat/9610012.
- [21] F. Wilczek, *Fractional Statistics and Anyon Superconductivity* World Scientific, Singapore (1990).
- [22] S. Sachdev, Phys. Rev. B **55**, 142 (1997).
- [23] V.P. Spiridonov and F.V. Tkachov, Phys. Lett. B **260**, 109 (1991).
- [24] L.P. Kadanoff and G. Baym, *Quantum Statistical Mechanics*, Benjamin, New York (1962).
- [25] P.M. Morse and H. Feshbach, *Methods of Theoretical Physics*, McGraw Hill, New York (1953), Chapter 10.
- [26] J. Callaway, *Quantum Theory of the Solid State*, Academic Press, New York (1974), Section 7.2.
- [27] A.V. Chubukov, S. Sachdev and J. Ye, Phys. Rev. B **49**, 11919 (1994).
- [28] R.E. Prange and L.P. Kadanoff, Phys. Rev. **134**, A566 (1964).

FIGURES

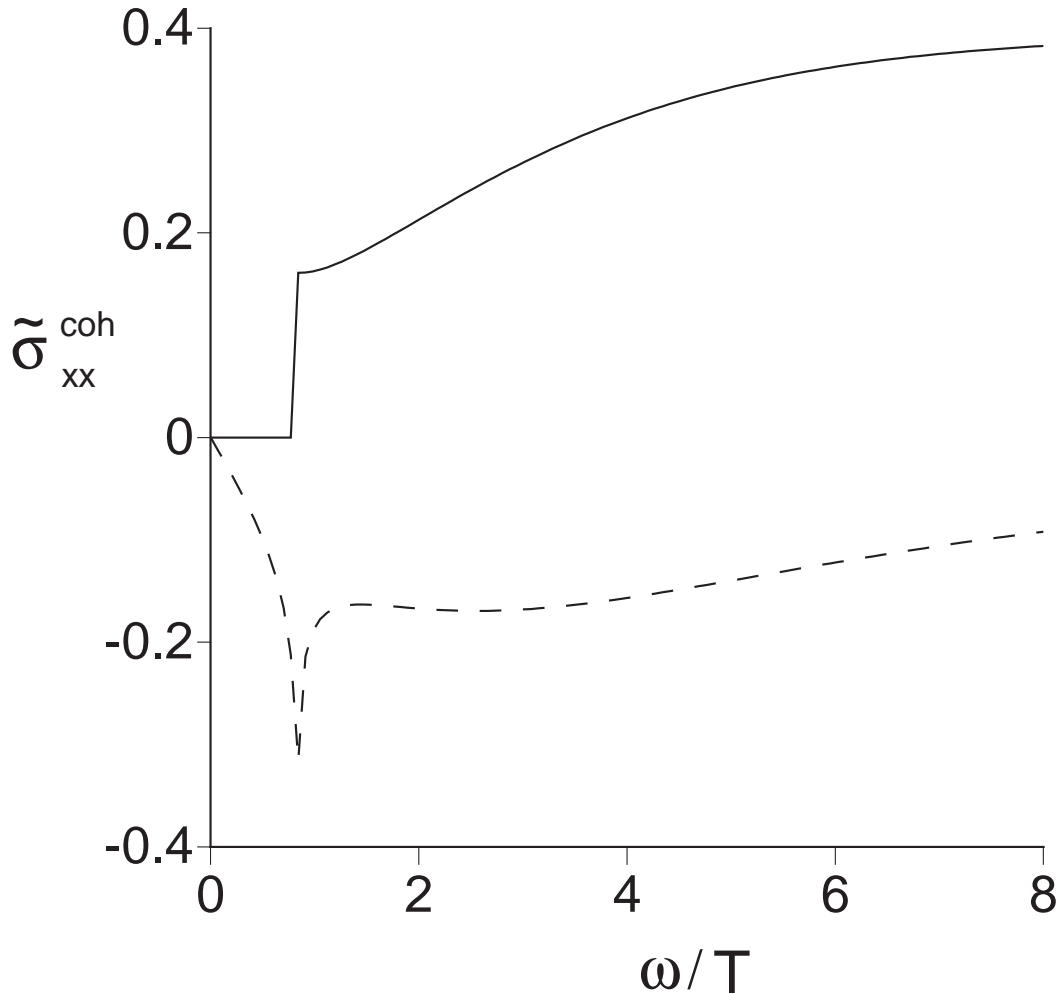


FIG. 1. Real (full line) and imaginary (dashed line) parts of the perturbative result (3.15) for the conductivity $\tilde{\sigma}_{xx}^{\text{coh}}(\omega)$ as a function of ω/T evaluated at $\alpha = 0.3$. The conductivity is measured in units of q^2e^2/h . The singularity is at $\omega = 2M(T)$, and is artifact of the absence of damping at this order. Note, as in (3.12), the conductivity $\tilde{\sigma}_{xx}$ contains another quasiparticle/quasihole contribution which is a delta function in the perturbative approach.

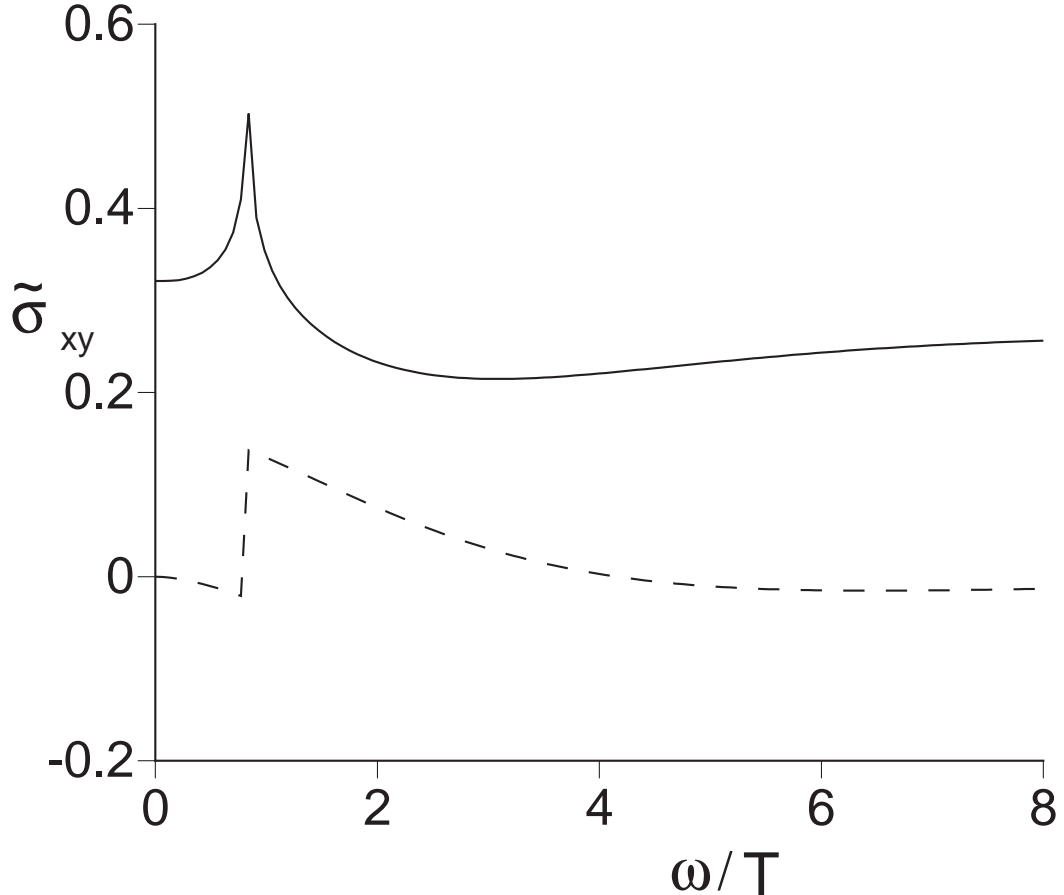


FIG. 2. Real and imaginary parts of the perturbative results for the Hall conductivity (3.19), (3.23) and (3.24) for $\tilde{\sigma}_{xy}(\omega) = \tilde{\sigma}_{xy}^{(1)} + \tilde{\sigma}_{xy}^{(2)} + \tilde{\sigma}_{xy}^{(3)}$ as a function of the ω/T evaluated at $\alpha = 0.3$. The conductivity is measured in units of q^2e^2/h . Again the spurious singularities are at $\omega = 2M(T)$. Note that unlike, $\tilde{\sigma}_{xx}$, the Hall conductivity is adequately described by the perturbation theory.

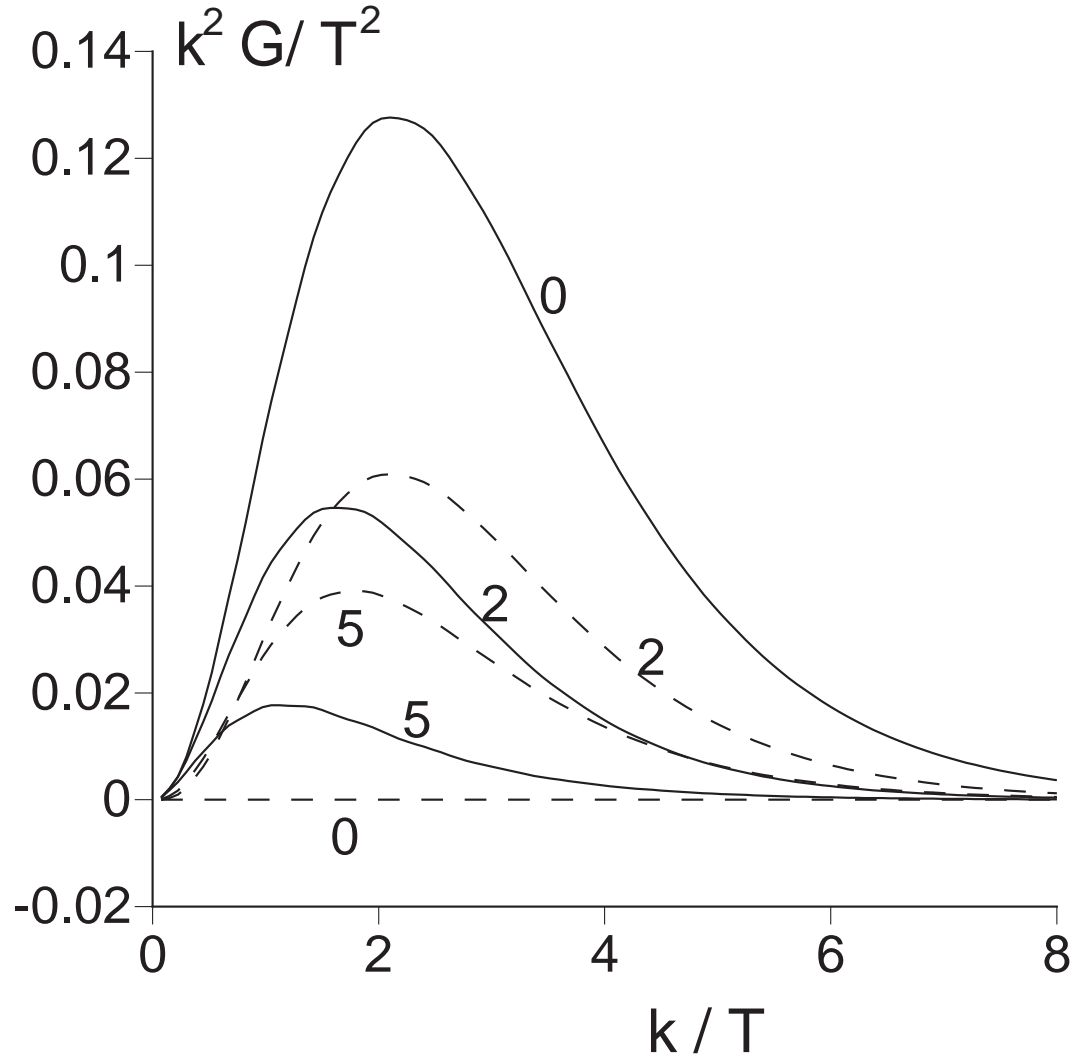


FIG. 3. Real and imaginary parts of the solution for the universal function k^2G/T^2 , introduced in (4.25), as a function of k/T for a few values of ω/α^2T . The combination k^2G/T^2 is that appearing in the integrand of the integral (4.27) for the conductivity.

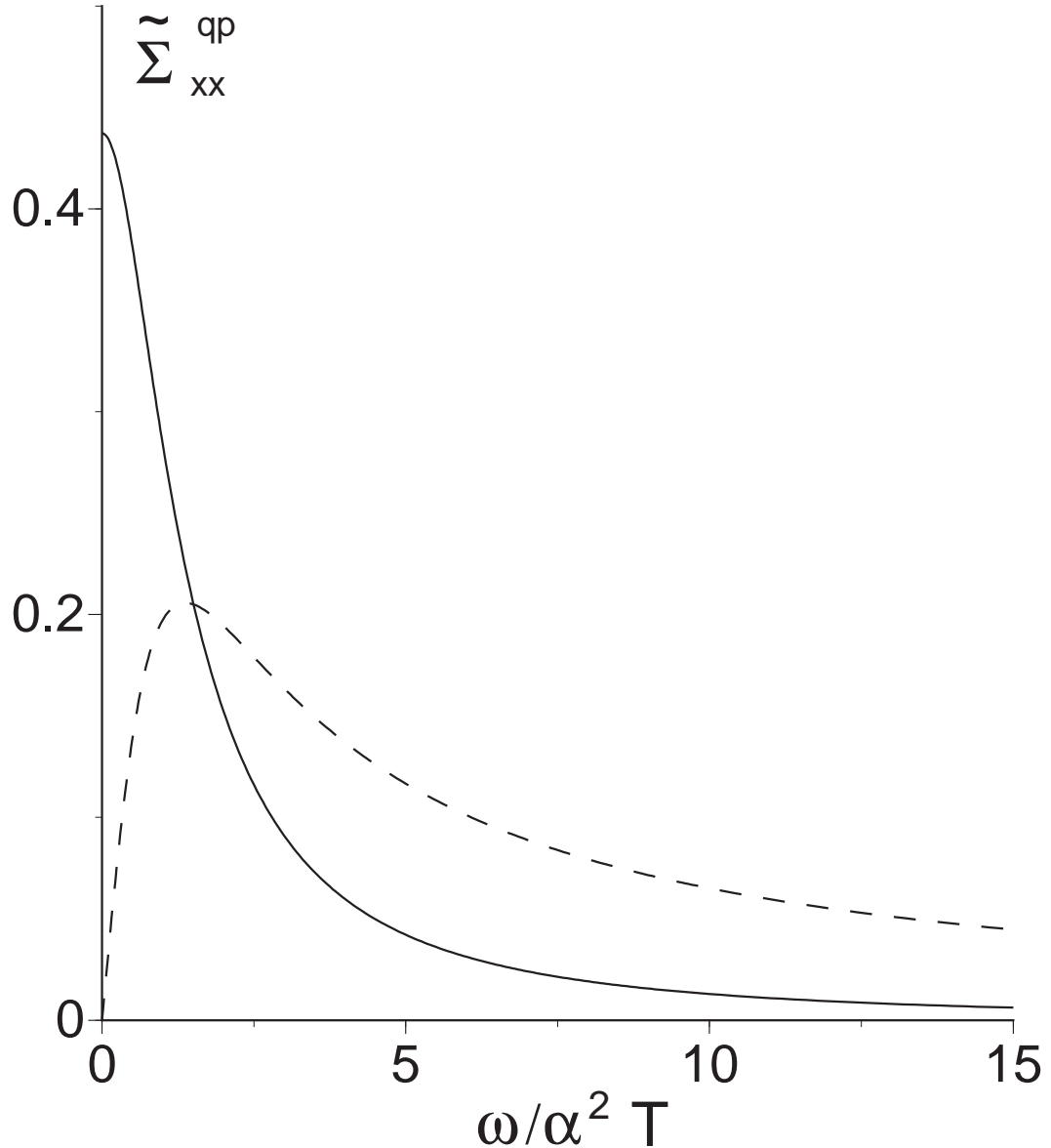


FIG. 4. Real and imaginary parts of the universal function $\tilde{\Sigma}_{xx}^{qp}$ as a function of $\omega/\alpha^2 T$. This result is related to $\tilde{\sigma}_{xx}^{qp}$ by (4.26).

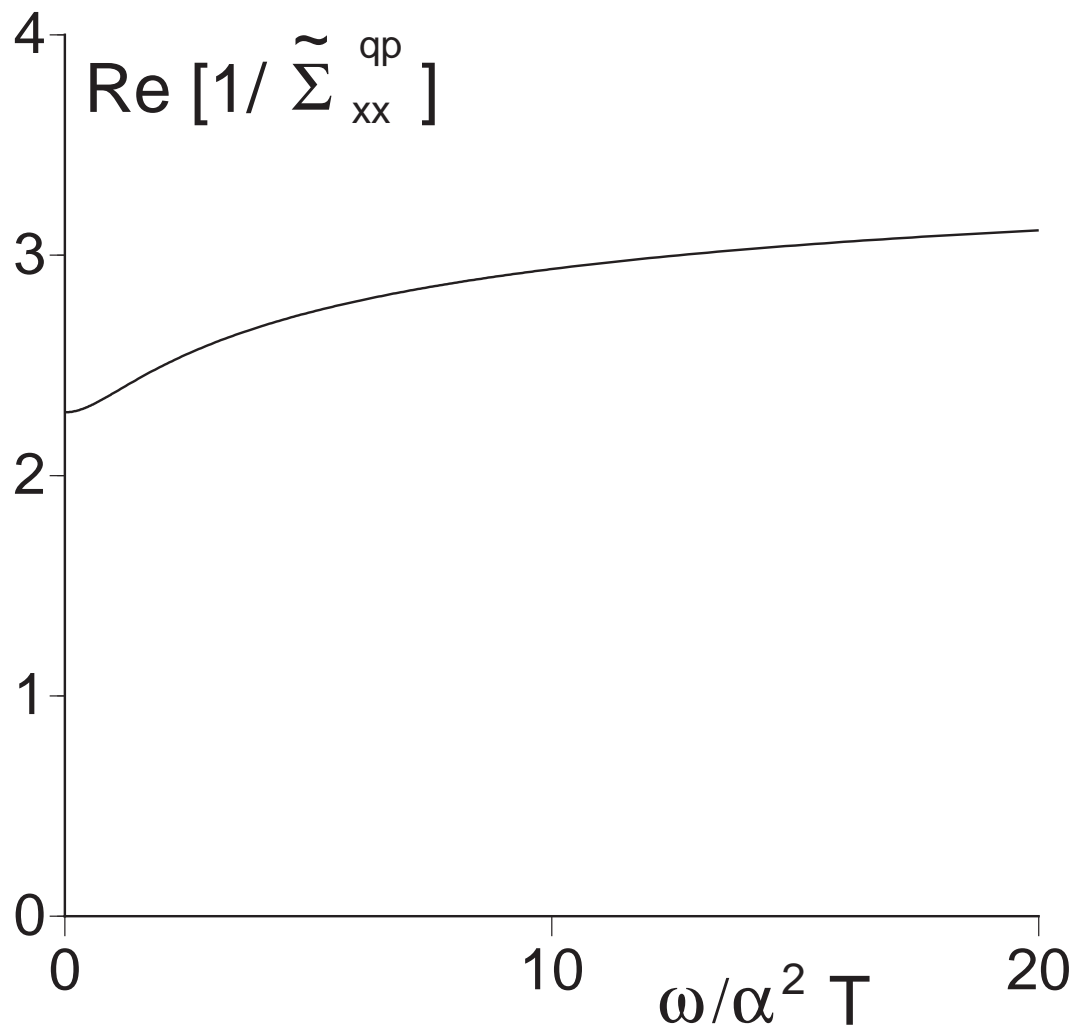


FIG. 5. Real part of $1/\tilde{\Sigma}_{xx}^{qp}$ as a function of $\omega/\alpha^2 T$.

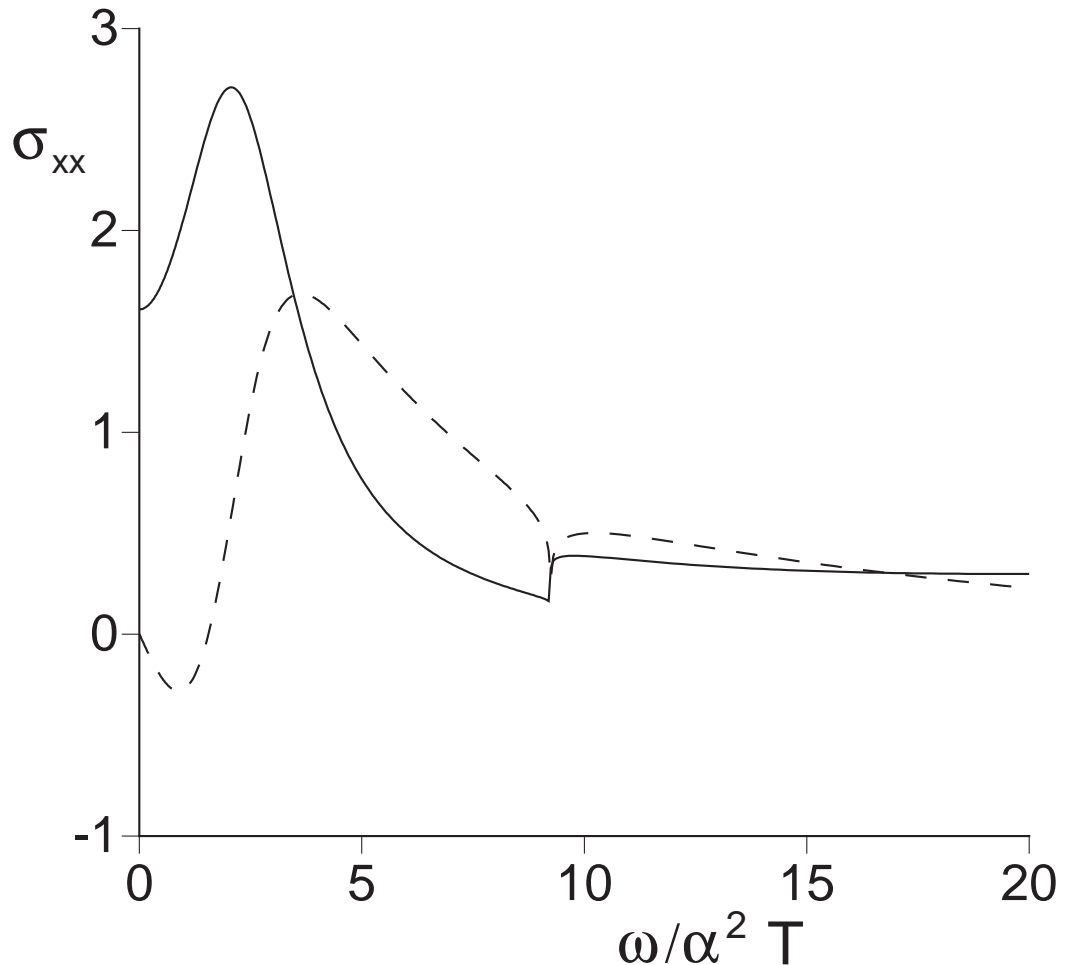


FIG. 6. Real and imaginary parts of the σ_{xx} as a function of $\omega/\alpha^2 T$, plotted at $\alpha = 0.3$. The conductivity is measured in units of $q^2 e^2/h$. The singularities at $\omega = 2M(T)$ ($\omega/\alpha^2 T \approx 9.2$) will be rounded out at higher orders.

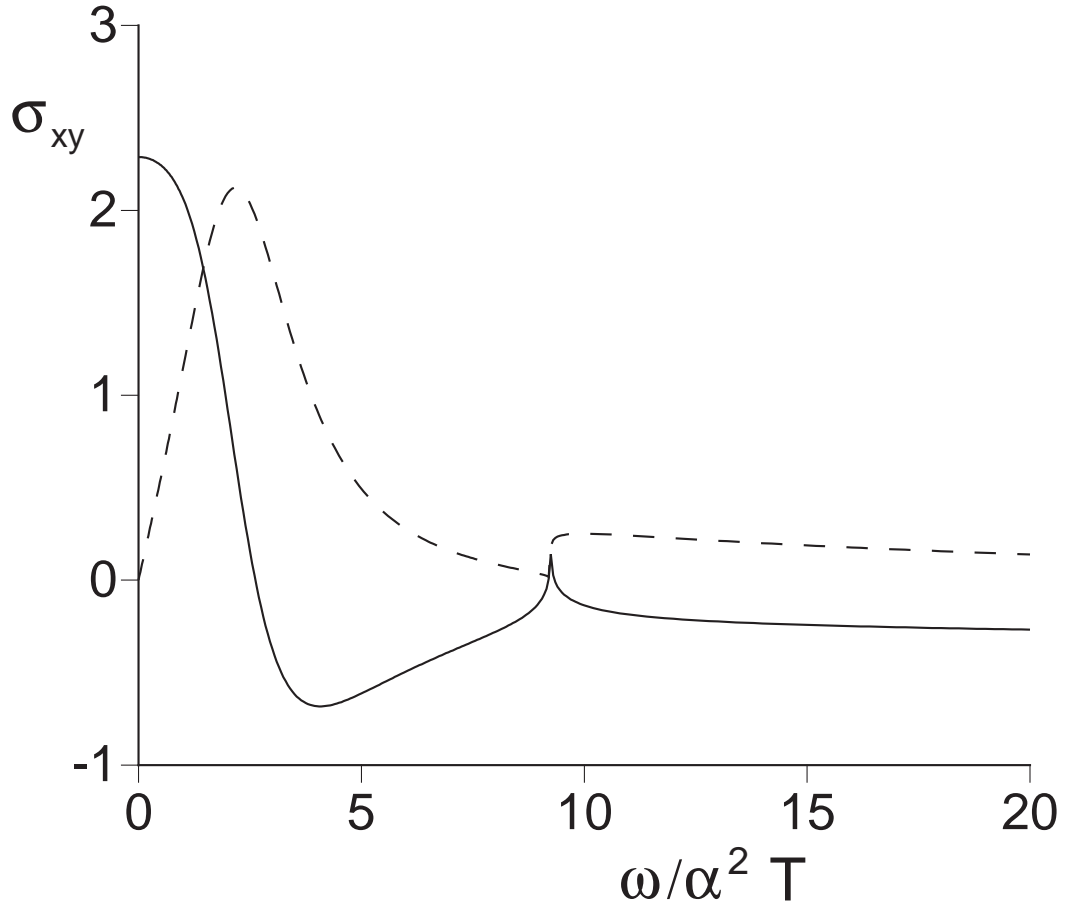


FIG. 7. Real and imaginary parts of the σ_{xy} as a function of $\omega/\alpha^2 T$, plotted at $\alpha = 0.3$. Again, the conductivity is measured in units of $q^2 e^2/h$ and the singularities at $\omega = 2M(T)$ ($\omega/\alpha^2 T \approx 9.2$) will be rounded out at higher orders.